PID AND LQR CONTROL OF A PLANAR HEAD STABILIZATION PLATFORM

A THESIS SUBMITTED TO
THE GRADUATE SCHOOL OF NATURAL AND APPLIED SCIENCES
OF
MIDDLE EAST TECHNICAL UNIVERSITY

BY

EMRE AKGÜL

IN PARTIAL FULFILLMENT OF THE REQUIREMENTS
FOR
THE DEGREE OF MASTER OF SCIENCE
IN
ELECTRICAL AND ELECTRONICS ENGINEERING

SEPTEMBER 2011

Approval of the thesis:

PID AND LQR CONTROL OF A PLANAR HEAD STABILIZATION PLATFORM

submitted by **EMRE AKGÜL** in partial fulfillment of the requirements for the degree of **Master of Science in Electrical and Electronics Engineering Department, Middle East Technical University** by,

Prof. Dr. Canan Özgen _____
Dean, Graduate School of **Natural and Applied Sciences**

Prof. Dr. İsmet Erkmen _____
Head of Department, **Electrical and Electronics Engineering**

Asst. Prof. Dr. Afşar Saranlı _____
Supervisor, **Electrical and Electronics Engineering**

Examining Committee Members:

Prof. Dr. Aydan Erkmen
Electrical and Electronics Engineering Dept., METU _____

Asst. Prof. Dr. Afşar Saranlı
Electrical and Electronics Engineering Dept., METU _____

Prof. Dr. M. Kemal Leblebicioğlu
Electrical and Electronics Engineering Dept., METU _____

Asst. Prof. Dr. Emre Tuna
Electrical and Electronics Engineering Dept., METU _____

Asst. Prof. Dr. Yiğit Yazıcıoğlu
Mechanical Engineering Dept., METU _____

Date: _____

I hereby declare that all information in this document has been obtained and presented in accordance with academic rules and ethical conduct. I also declare that, as required by these rules and conduct, I have fully cited and referenced all material and results that are not original to this work.

Name, Last Name: EMRE AKGÜL

Signature :

ABSTRACT

PID AND LQR CONTROL OF A PLANAR HEAD STABILIZATION PLATFORM

Akgül, Emre
M.S., Department of Electrical and Electronics Engineering
Supervisor : Asst. Prof. Dr. Afşar Saranlı

September 2011, 84 pages

During the uniform locomotion of legged robots with compliant legs, the body of the robot exhibits quasi-periodic oscillations that have a disturbing effect on different on-board sensors. Of particular interest is the camera sensor which suffers from image degradation in the form of motion-blur as a result of this camera motion. The effect of angular disturbances on the camera are pronounced due to the perspective projection property of the camera. The thesis focuses on the particular problem of legged robots exhibiting angular body motions and attempts to analyze and overcome the resulting disturbances on a camera carrying platform (head). Although the full problem is in 3D with three independent axes of rotation, a planar analysis provides significant insight into the problem and is the approach taken in the thesis. A carefully modeled planar version of an actual camera platform with realistic mechanical and actuator selections is presented. Passive (filtering) and active (controller) approaches are discussed to compensate/cancel motion generated disturbances.

We consider and comparatively evaluate PID and LQR based active control. Since PID has the limitation of controlling only one output, PID-PID control is considered to

control two states of the model. Due to its state-space formulation and the capability of controlling an arbitrary number of states, LQR is considered.

In addition to standard reference signals, Gyroscope measured disturbance signals are collected from the actual robot platform to analyze the bandwidth and test the performance of the controllers. Inverted pendulum control performance is evaluated both on a Matlab-Simulink as well as a precise electro-mechanical test setup. Since construction of the planar head test setup is in progress, tests are conducted on simulation.

Keywords: Legged Robots, Camera Platform Stabilization, PID Control, LQR Control

ÖZ

PID VE LQR YÖNTEMLERİ ILE TEK EKSENLİ KAFA STABİLİZASYON PLATFORMU KONTROLU

Akgül, Emre
Yüksek Lisans, Elektrik ve Elektronik Mühendisliği Bölümü
Tez Yöneticisi : Yrd. Doç. Dr. Afşar Saranlı

Eylül 2011, 84 sayfa

Bacaklı robotların gövdeleri robotların yürüme hızına bağlı olarak belli bir salınım yapar. Bu salınım yüzünden algılayıcılardan ve özellikle kameradan veri almak zorlaşmaktadır ve görüntü kalitesini bozan unsurlar oluşmaktadır. Bu çalışmanın amacı, çeşitli salınım izolasyon yöntemlerini kullanalarak bahsedilen salınımları yalıtacak bir kamera (kafa) stabilizasyon sistemi tasarlamaktır. Problemin genel tanımı 3 eksende olsa da, sistemin tek eksende analizi çözüme yonelik önemli sonuçlar doğuracaktır ve tez kapsamında tek eksenli bir kafa stabilizaston sistemi tasarlanmış ve kontrol edilmiştir. Bu amaç çerçevesince, kafa platformunu kontrol etmek için farklı kontrolculer denemiş ve bunlarun uygunluğu karşılaştırılmıştır. Tek eksenli kafa modeli mekanik ve eyleyici detayları da hesaba ayrıntlı bir şekilde katılarak, tasarlanmış ve modellenmiştir. Pasif(izolator) ve aktif(kontrolcü) salınım izolasyon methodları, robot hareketinden kaynaklanan salınımları etkisiz hale getirmek için denenmiştir.

PID ve LQR kontrolcüler ayrı ayrı denenmiş ve performans karşılaştırmları yapılmıştır. Öncelikle PID kontrol denenmiş ancak bu methodun sistemin sadece tek değişkenini

kontrol edebiliceğinden, çift PID-PID yapısına geçilmiştir. Bunun yanı sıra aynı anda sistemin pek çok değişkenini kontrol edebilme yetisine sahip olan LQR kontrolcü de denenmiştir.

Standart referans sinyallerinin yanı sıra, gyroskop kullanılanarak robot deneyleri sırasında alınmış, açısal hız sinyalleri de kontrolcülerin performans analizi sırasında kullanılmıştır. Ters sarkaç modeli hem Matlab-Simulink ortamında hem de üretilmiş olan bir deney platformunda denenmiştir. Kafa sisteminin üretimi halen devam etmekte olduğundan, ilgili deneyler simulasyon ortamında denenmiştir.

Anahtar Kelimeler: Bacaklı Robotlar, Kamera Platformu Stabilizasyonu, PID Kontrol, LQR Kontrol

to my loving mother
and to the memory of my father,

ACKNOWLEDGMENTS

I would like to express my deep appreciation and sincere gratitude to my supervisor Dr. Afşar Saranlı for his leading guidance, encouragement, and continuous support from beginning to the end of my M.S. study. His suggestions during our research meetings played a tremendous role in helping me to broaden my view and knowledge. He showed me different ways to approach a research problem and the need to be persistent to accomplish any goal. He let me take part in the SensoRHex project which was a great opportunity for me to extend my academic and technical skills. He also made the Rolab (Laboratory of Robotics and Autonomous Systems) a wonderful workplace by providing us many new equipments we need.

I should also extend my sincere thanks to Dr. Yiğit Yazıcıoğlu for his help on pointing out the problems occurred during my study and proposing solutions especially in modeling and control part of my work.

I wish to express my deep sense of gratitude to Dr. Uluç Saranlı for his guidance and being a source of inspiration for me in the conduct of my thesis work and our research project. I also would like to thank Dr. Kemal Leblebicioğlu for conducting the ULİSAR project in the Rolab which added much to my experience.

I literally consider myself a lucky person to work with the amazing group of people in Rolab. I am very thankful to Mert Ankaralı, Emre Ege, Orkun Öğücü, Ferit Üzer, Gökhan Koray Gültekin, Babak Rohani and all other members for sharing me their time and knowledge. Further thanks should also go to the all members of BDRL (Bilkent Dexterous Robotics and Locomotion).

I would like to thank the Scientific and Technological Research Council of Turkey (TÜBİTAK) for awarding me their prestigious master of science studies scholarship.

I apologize from the people who I should also have included their names here for their contributions but may forgot because of the rush I am in. I send my thanks to all

individually.

Finally, yet the most importantly, nothing is adequate to express my heartfelt feelings to my beloved family forever. None of this would have been even possible without the love and patience of them. I owe a great many thanks to my loving mother(Gülay Akgül) for her undying love, unconditional support, encouragement and her trust in me. And my deep regards to the memory of my father (Ali Akgül) whom i follow since and always.

TABLE OF CONTENTS

LIST OF TABLES

TABLES

LIST OF FIGURES

FIGURES

PID	Proportional-Integral-Derivative
LQR	Linear Quadratic Regulator
θ	Angle of Pendulum
x_c	Position of Pendulum Cart
ϕ	Angle of Head Stabilization Platform
s	Actuator Length of Head Stabilization Platform
α	Actuator Angle of Head Stabilization Platform
γ	Angle of Force Actuation to the Head Stabilization Platform
K_P	Proportional Control Constant of PID Control
K_I	Integral Control Constant of PID Control
K_D	Derivation Control Constant of PID Control
Q	Weight Control Parameter in LQR Control
R	Control Effort Parameter in LQR Control

CHAPTER 1

INTRODUCTION

1.1 Motivation

Different types of mobile platforms are in use today. Tracked or wheeled vehicles have been around for a long time. Although these platforms ensures high speed, robustness and easiness of use, they are capable of locomotion mainly in relatively flat environments. In other words their performances are restricted to the environment for which they are built. Disadvantages of wheeled platforms must be discussed in a comparison to legged platforms. In [16] and [34] legged robots are investigated in terms of advantages to the wheeled robots. As the application fields of robotics increase, need of robots that can operate in unstructured and rugged environmental conditions gradually arises. Mobile robots with tracks or wheels result in over-sized designs when they are built to meet the demands of the terrain. Still a large percentage of the land mass of the Earth is still accessible only to legged biological creatures. At various scales from insects to very large mammals, these show a striking ability for high speed, energy efficient locomotion on practically any terrain. Legs also show functional diversity, being used for other purposes than locomotion alone.

Although wheeled and tracked systems still dominate today, these examples in nature make the study of legged robot designs a necessity for the ultimate performance of future systems. Moreover, a number of examples from the scientific and commercial domain such as the RHex [37] and BigDog[28] morphologies demonstrate that impressive locomotion performance can be achieved by engineering systems by carefully and selectively borrowing principles from the nature. In these two examples, the main principles are significant leg compliance, dynamic stability and control; resulting in a

high speed, dynamically stable gait with minimal mechanical complexity.

Many different motion capabilities are admitted by dynamically stable legged morphology such as, running [7], leaping and self-righting [35], jumping and stair climbing. Also by using legs in different functional roles, other tasks which would require other specialized structures on wheeled robots, can be achieved. E.g., legs can be used to push/pull objects or orient sensors in different directions. Another biologically inspired hexapod robot example is the RISE robot that has the capability of climbing vertical structures like walls and trees [39, 36, 8]. A variant of the RHex morphology, the SandBot is tuned and has special leg designs to move successfully and efficiently on the sand [18].

Although it is acceptable to say legged robots have a potential for greater mobility than wheeled and tracked robots, and on many different terrains like, designing and controlling legged robots exhibit many unique difficulties. In wheeled robots in order to give actuation to the system, there exists only a motor, gearbox and wheel structure, resulting in a very simple and robust system. For most of the legged robots, designed for a statically stable locomotion mode, there exists complex mechanical designs and a greater number of actuators. Many different leg mechanisms are used to move certain legs while other legs keep the robot stable on the ground by keeping the robot Center-of-Gravity (GOG) within the leg support triangle. In a common legged robot design, each leg consists of at least two actuators in order have more freedom during locomotion. Resulting kinematic complexity result in robots that are often slow (due to higher gear reduction ratios) and fragile beating the original motivation of locomotion on rugged terrain. Reducing the number of actuators with a simpler design results in much faster and more rugged designs but the reduced degrees of freedom and increased speed requires the robots to be dynamically balanced, hence requiring high bandwidth active control for successful locomotion. Some rare designs such as the RHex morphology exhibit self stable behavior that can partially lift the need for active control for certain locomotion behaviors and enable open-loop control.

Our legged robotic research platform SensoRHex has the original RHex morphology with only one actuator for each to its legs. This results in a great simplification in actuation and mechanical design and low level control of the legs. However, gait level

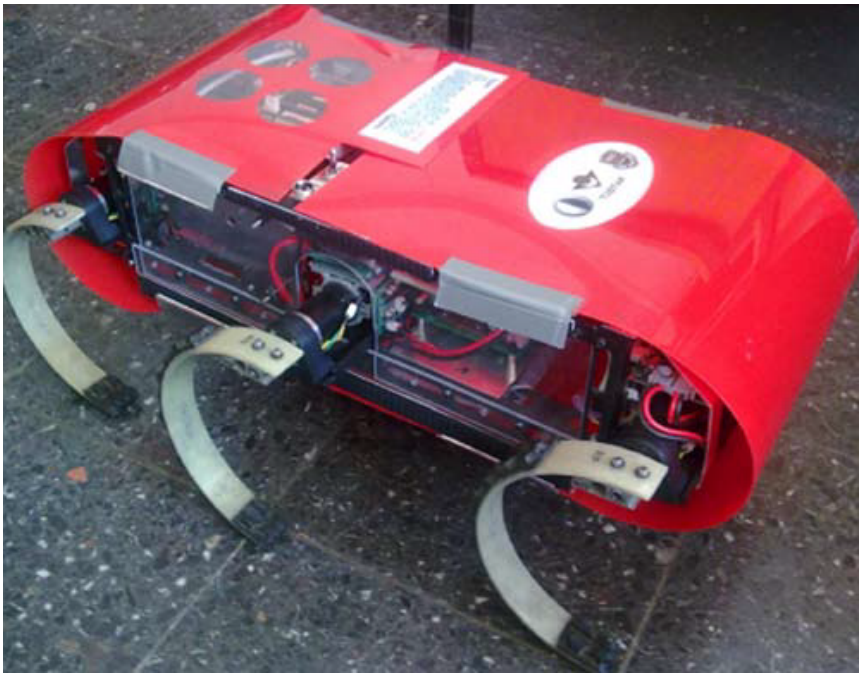

Figure 1.1: C Shaped Legs of SenoRHex Robot in METU Electrics and Eletronics Department.

control of various dynamic behaviors is an active area of research. SensoRHex legs are C-shaped composite curved beams as illustrated in Fig. 1.1. These composite structures act like as a spring-damper system.

The body moving on these composite legs based on a given gait pattern results in complex oscillations in the body. One of the main objectives of our research group is to build autonomous legged robots which integrate data from a variety of on-board sensors in order to accomplish high level behaviors. Unfortunately, most sensor data is disturbed or corrupted by high frequency mechanical vibrations as well as by motion exceeding certain magnitude and frequency occurs due to the legged locomotion.

Of particular interest for us is the visual sensor (camera) mounted on the robot body. In particular, a distortion known as motion-blur occurs when camera moves with respect to the scene being imaged. For a scene at a reasonable distance, rotational motion of the camera dominates as the source the motion-blur distortion. In nature, fast moving animals have their important sensors (eyes, inner ears as effective inertial sensors) placed on a stabilized head. The inspection of their motion illustrates that although the head still is subject to translational up-down motion, the angle of the

head is tightly controlled.

Therefore, stabilizing the camera carrying platform becomes a particularly important problem for fast moving, dynamically stable legged robots.

A camera stabilization platform that we sometimes refer as a *head* is suggested in order to overcome the visual sensor motion-blur problem. We postulate that this platform will eliminate high frequency oscillations by using passive vibration isolators. The legs which are themselves spring-damper systems also pre-filter the original disturbances from the ground. We are hence motivated to investigate the feasibility of canceling the remaining low frequency quasi-periodic oscillations by active angular control of the platform. We use off-the-shelf linear DC motors and investigate actual feasibility of such control based on realistic parameters of the model.

Our strong motivation is that this platform carrying the camera, when coupled with a successful control algorithm will bring the angular motions within the tolerances of the camera, hence resulting in better vision data quality. The visual data quality is important because it effects the performance of many vision based perception algorithms such as object detection and recognition, pose and state estimation and ultimately all high level behaviors.

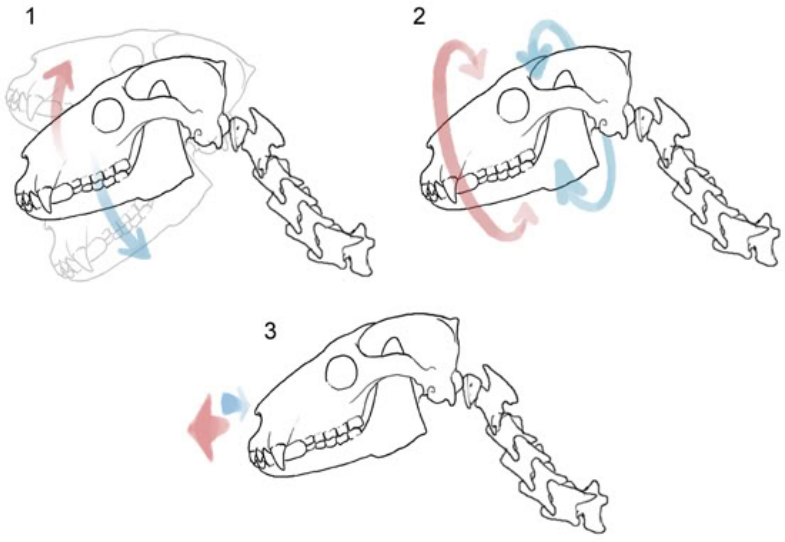

Figure 1.2: Head movements in an Animal Skeleton System [2] : (1) Pitch, (2) Roll and (3) Yaw.

The design of the full camera carrying platform has the ability to move in pitch, roll and yaw axes as illustrated in Fig. 1.2 for a biological example of an animal skeletal head. Angular disturbances coming from our robot body effect all three of these axes and hence the platform needs to be controlled on all three axes so it can compensate disturbances due to motion of the robot platform.

However this concept is not a totally new concept. Generalization of camera stabilization could be mentioned as platform stabilization. Researches about platform stabilization is conducted about 100 years. Stabilization platforms are used to stabilize a board array of sensors, cameras, harddisk drives, telescopes, antennas, hand cameras and weapon systems. So the application of this area is used by scientific,commercial and military purposes for several times. For example; surveillance, gun-turret control, communications,astronomical telescopes [10], cameras [41], improving gunfire performance [31]. Even Hubble Space Telescope works with the help of this technology. Furthermore stabilization platforms are mainly used in all kind of vehicles such as, ground vehicles, ships , aircrafts and spacecrafts.

As a start we discuss the suitability and comparatively present the performances of two different control strategies to control the angular velocity of the camera/head stabilization platform. The first method is the common Proportional-Integral-Derivative (PID) control. Due to its state-space formulation and the capability of controlling an arbitrary number of states, the Linear Quadratic Regulator (LQR) is evaluated last to control all states of the inverted pendulum.

1.2 Methodology

Before designing any hardware for the control of the camera platform, firstly the mathematical model of the system must be derived and a series of simulations must be conducted in order to assess the feasibility of the design. All simulations of the system are implemented in Matlab-Simulink environment by utilizing the manufacturer provided system model.

In accordance with our motivation of ultimately controlling a particular three-axis platform design and actuator configuration, the thesis then considers a planar ap-

proximation to this platform with a single actuator. This simplification still preserves important properties of the problem while avoiding some of the model complications. The thesis approach is to consider realistic disturbances on a single axis initially and achieve acceptable control before moving into multiple axis control as future work.

For the planar platform, the nonlinear state-space model is derived and a Simulink model is constructed. This model is used to simulate the behavior of the system. Since the actual planar test setup is not ready, this part of the thesis is limited to simulation results. Nevertheless, we select all simulation model parameters in accordance with our mechanical design and actuator choices available for this design. In fact, the simulations act as a tool for both actuator and control approach selection for the design.

As part of our methodology, PID and LQR based control approaches are considered to stabilize both systems. Thir nonlinear models are later linearized using Taylor Series expansion in order to design the necessary LQR control parameters. PID controllers on the other hand are experimentally tuned.

1.3 Contributions

Stabilization platforms are most big in size, such as telescope stabilization platforms, gun-turret stabilization platforms, antenna-radio stabilization platforms, camera stabilization platforms for UAV's. However our design must fit into our robot RHex. That constraint forces us to produce one of the smallest camera stabilization platform in the literature. Although a 3D platform is produced ,this study investigates characteristics and controllability of a single axis camera stabilization platform. So we can control our 3D model better with the experience gained from single axis stabilization platform.

In order to stabilize a platform mainly two approaches are considered; gimbal and stewart platform. However our motivation is based on an original platform stabilization configuration which is a simplified steward platform with three actuators. By a certain combination of actuators pitch, yaw and roll motion can be obtained with the help of linear DC motor. This three actuated approach to the stewart platform is a

totally new concept in platform stabilization.

An important evaluation is the evaluation of a specific platform/actuator configuration that will be used in practice and also explicitly modeling a particular platform design that we will use in practice.

A comparative evaluation of two popular control approaches as a baseline approach in controlling our realistic system as well as an actual hardware inverted pendulum. A detailed analysis of PID(Proportional Integral Derivative) and LQR(Linear Quadratic Regulator) controller is given. Moreover, we investigate LQR tuning in relation to actuator capabilities. We take into account actuator limitations in the form of actuator saturation and use these results for actuator selection.

In addition, presence and consideration of realistic disturbance signals collected from the actual robot platform during locomotion at different speeds. And consideration of how these can be integrated into the simulation model is included.

Moreover the link between controller performance of the robot camera stabilization platform and motion blur on the image that is retrieved on the robot is created. And ideas about a higher quality image set is given.

1.4 Outline of the Thesis

Thesis starts with an introduction chapter in which, the aim and purpose of the study is described including motivation and contribution. And following chapter is devoted to the existing work on head stabilization platform.

The third chapter discusses all theoretical background used during the implementation of the platforms. And fourth chapter introduces the simulation and hardware designs of the platforms.

Chapter 5 gives simulation results of the head stabilization platform. Results of different experiments are given with a comparative approach.

Finally the conclusion is given with the predicted future work at chapter 6.

CHAPTER 2

LITERATURE SURVEY

Stabilization platforms are used to stabilize a board array of sensors, cameras, hard disk drives, telescopes, antennas, hand cameras and weapon systems. The research about these platforms is conducted about 100 years. So the application of this area is been used by scientific,commercial and military purposes several times. For example; surveillance, gun-turret control, communications, astronomical telescopes [11] , cameras, improving gunfire performance[41]. Even Hubble Space Telescope works with the help of this technology.Furthermore stabilization platforms are mainly used in all kind of vehicles such as, ground vehicles, ships , aircrafts and spacecrafts. The main idea between this concept is hold or control the line of sight of the sensor which is used.

Figure 2.1: Camera stabilization platform mounted on unmanned air vehicle [1].

Moreover cameras mounted on any kind vehicles such as ground,air,sea even space, uses stabilization platforms in order to obtain better resolution for surveys of the

environment. [41] investigates the problem in order to create a solution for video tele-operated ground vehicles. During motion in violent terrains image is tried to be stabilized by using a system that counteracts the movements of the vehicle body. Also unmanned air vehicles uses the camera stabilization technology during image retrieving for surveilance purposes with great efficiency as seen in Fig. 2.1. Also [29] gives detailed information about optical imaging systems on stabilization platforms.

[14] investigates the same problem for antennas mounted on mobile vehicles. Since for a high quality satellite communication the antenna must be pointed to the satellite with an accuracy of one degree position of the antenna must be aligned accurately during locomotion of the vehicle. Fig. 2.2 shows the picture of a satellite antenna installed on a 4x4 test vehicle in order to determine the off-road performance of the stabilization system.

Figure 2.2: Antenna platform mounted on 4x4 vehicle [14].

Another example for stabilization platform could be given as gun turret stabilization. One of the most important capabilities of today's turret subsystems is the fire on the move, which enables very high firing accuracy while moving on a rough terrain. This capability is obtained basically by gun stabilization, which means holding the orientation of the gun stationary relative to a reference on the ground even under random disturbances generated by the vehicle moving on an unconstrained terrain [32].

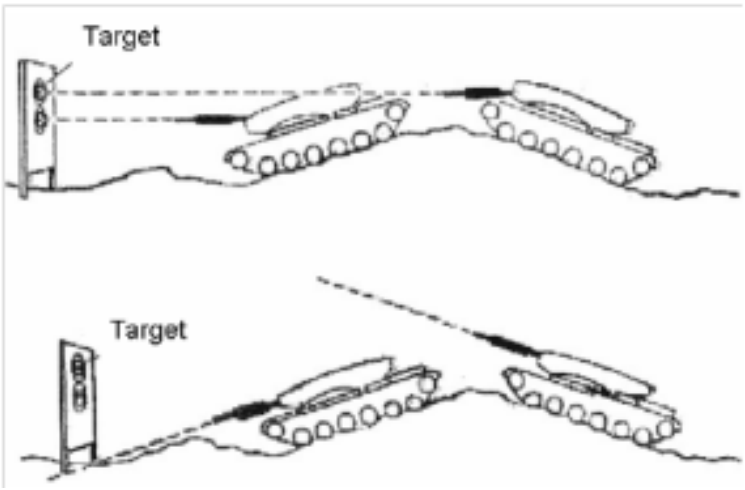

Figure 2.3: Gun stabilization on elevation axis[32].

In today's stabilization systems, holding the turret orientation stationary on the target is not enough because most of the targets do poses also "fire on the move" capability. The time for aiming and shooting has been greatly reduced, so there is a need for target tracking and fast reaction. Stabilization systems having target tracking capability are called third generation stabilization systems. In this generation, unbalance compensation using accelerometers are used in addition to disturbance feed-forward technique because most of the turret subsystems using third generation stabilization systems have huge guns (120mm and 140mm guns for main battle tanks) resulting in high mechanical unbalances [17].

Also this approach is used in vehicles in order to improve the ride quality and increase off-road mobility. Using active suspension controls the disturbance from the environment to the sensors are tried to be minimized [13]. Moreover active vibration isolation systems are used for rejection seismic level disturbances with satisfying results [12].

2.1 Stabilization Platform Methodology

There exists one main solution for this problem, to mount sensor or payload that will be stabilized,on a platform. Gimbals in Fig. 2.4 and stewart platforms in Fig. 2.5 are mainly selected in order to overcome the problem where the payload could be camera, antenna, IR detectors. More importantly those payloads requires stabilization

in terms of line-of-sight [23] and the amount of angular error in those applications must be around 6mdeg. However those platforms have great differences in mechanical structure however in certain applications they serve to the same purpose.

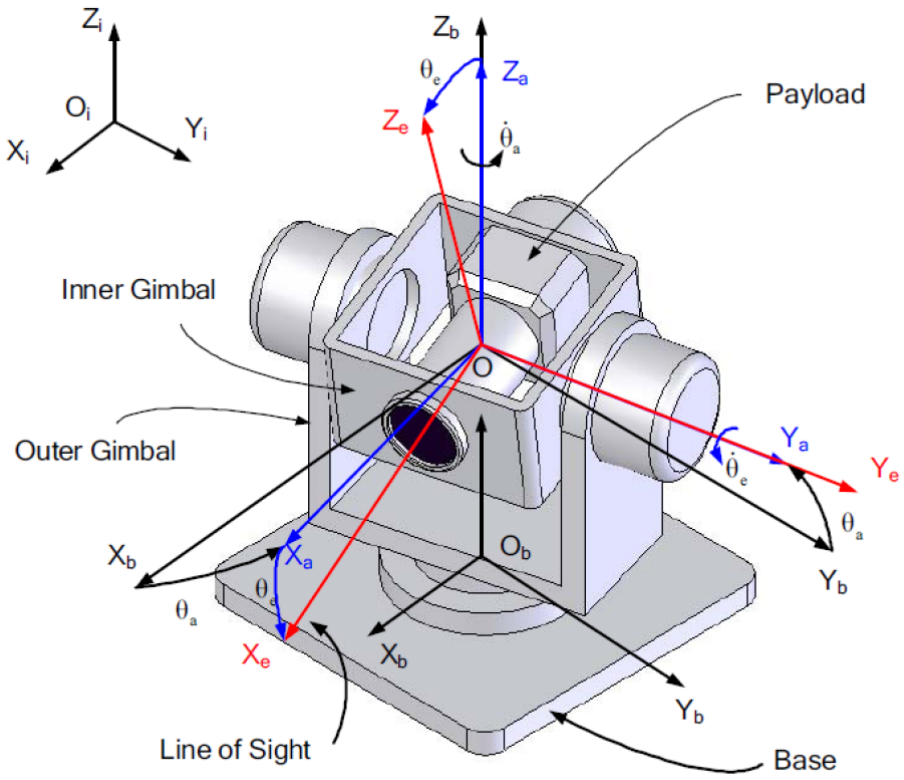

Figure 2.4: A Typical Two Axes Gimbal Mechanism [15].

Gimbal is referred as any type of mechanism that allows the line of sight of the object to be rotated or stabilized whereas originally gimbal was thought of a concentric set of rings suspended on bearing. Gimbal system is used as pointing and tracking applications in mostly unmanned aerial and grounded vehicles. Many studies are conducted about gimballed system over the year and advanced gimballed systems have control over all three rotational axis. However as the number of controlled axis increases the complexity of gimballed design increases exponentially. Though, two axis systems are more common in application. Like [44] two axes gimballed mechanism are used in order to create a stabilization platform.

Moveover stewart platform which is illustated in Fig. 2.5 is a combination of moving upper platform, fixed base and six actuators which connects the base and the platform.

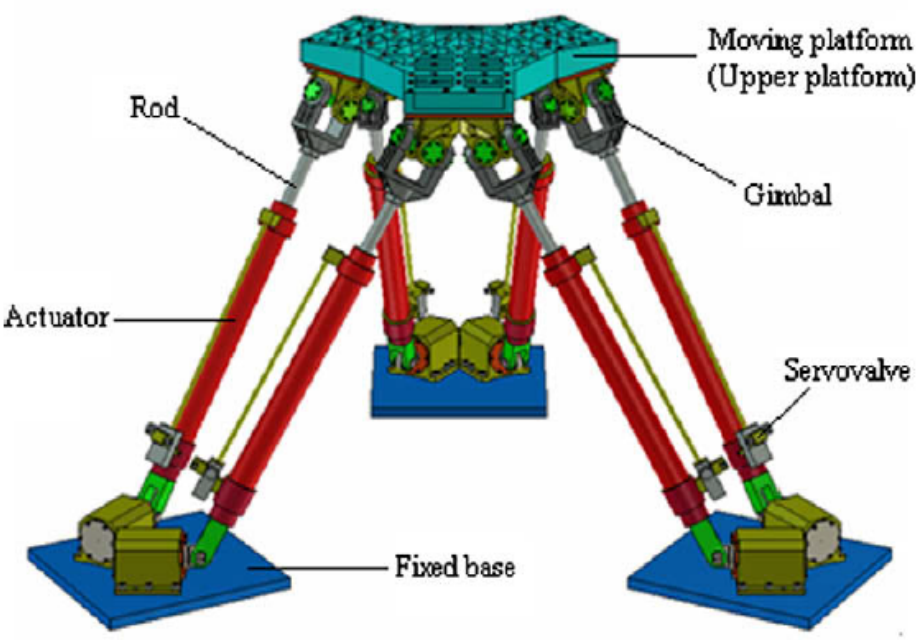

Figure 2.5: Configuration of 6-DOF Gough-Stewart Platform [42].

Although this platform has a more complex mechanical structure it has the ability of 6 degree of freedom motion which are three rotational and three translational motions which is impossible to be obtained by a gimballed system. Many ideas in different applications including our research interest are tested on this platforms. For example [22] deals with the position control of the stewart platform by using inverse dynamics control. Also [27] uses adaptive control for the sinusoidal disturbance cancellation in two axes, which method is also used in our study. [42] uses PID(Proportional Integral Derivative) and PDGC(Proportional Derivative Control Gravity Compensation) controllers to track a 6 DOF sinusoidal signal with the successful results shown in Fig. 2.6.

Furthermore another and simple approach is proposed. This method is called mirror stabilization, in which a mirror that is placed on the optical path of the sensor is stabilized, rather than mass stabilization of the entire assembly. A two-axis mirror-stabilized configuration (heliostat) is used by researchers with satisfying results [17].

As stated in Chapter 1 the main motivation behind the study is to implement a head stabilization platform where the camera of the robot will be mounted and by reducing the amount of angular velocity,increase in image data is proposed. However angular

velocity at our robot body (SensoRHex) due to legged locomotion is a three axes movement. So a gimballed mechanism which will compansate this motion will be too complex and the need of 6 DOF motion which stewart platform suggests will be needless. So an original platform stabilization model is suggested in this thesis which could be seen as a derivation of stewart platform with three actuators and a capability of 3 DOF motion.

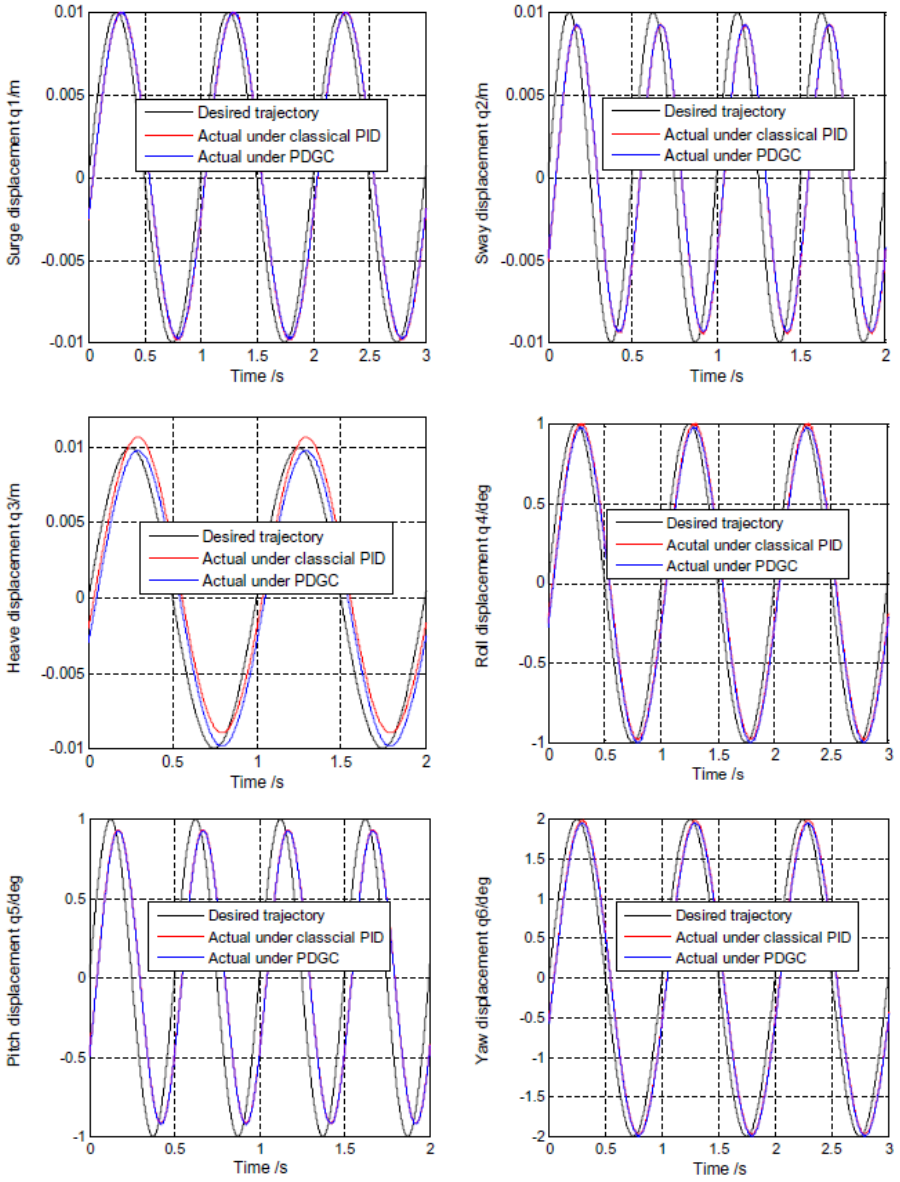

Figure 2.6: Configuration of 6-DOF Gough-Stewart Platform [42].

2.2 Controlling Approaches

In order to design an efficient control system, engineers mainly use both passive and active disturbance cancellation techiniques. As [12] states vibration isolation is done by using a suitable spring damper system then the residual vibrations are tried to be eliminated by using an active system which includes an actuator. The disturbances with high frequency and low amplitude will be eliminated by the passive isolation system. In our robot those disturbances occurs due to the structural issues. On the other hand active vibration cancel outs the movements with high amplitude and low frequency, in our case those vibrations occurs due to the legged locomotion of the SensoRHex. As seen in Fig. 2.7 undesired movements are firstly eliminated in passive vibration isolation state then active vibration cancellation system deals with the residual disturbance. Another practical application of this vibration cancellation method is also be given as the active vehicle suspension control in off road vehicles [13].

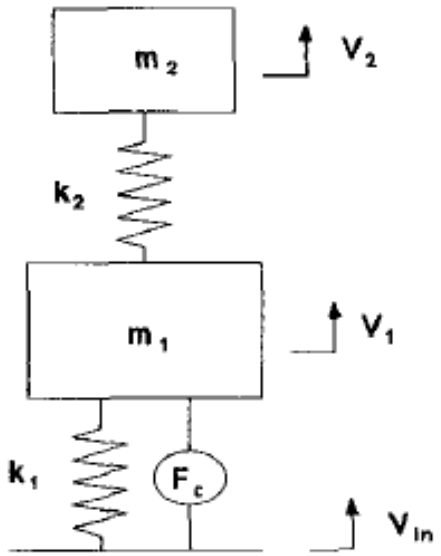

Figure 2.7: Comparison of LOS rate when control is and is not applied [12] .

Eventhough the requirements of every system differs from each other there are some basic principle for stabilizing a platform. The main principle is mass stabilization, this approach relies on equating the resultant torque on the system to zero. In other words measure and apply the disturbance torque to the platform in order to stabilize

it. By the help of the improvements in developing a reliable gyro, this method is very reliable and efficient. And so called active vibration isolation system.

Inspite of the fact that, traditional control techniques as P controller or PID controller gives good results with the help of more complicated control algorithms such as state variable feedback, adaptive techniques and disturbance observer design system performance can be improved significantly as explained in [19]. For instance [25] deal a nonlinear inertial stabilization system with an advanced self-tunning controller.

Also we have to note that sliding mode controller is a common and advanced controller which proves its effectiveness in various systems by different researchers. A smooth sliding mode controller is designed and tracking performance is discussed in [20] and [21] by using the stewart platform. [38] proposes a sliding mode controller for a gimballed mechanism which has an aim of stabilizing a flat antenna.

In [25] Li, Hullander and DiRenzo focuses on the disturbance rejection problem in gimbal mechanisms and proposes a Linear Quadratic Gaussian(LQG) control which is capable of estimating the disturbances. Fig. 2.8 is the angular rate of change in the line of sight at the instance when the disturbance occurs. Also they present a similar study in with a self tuning controller for inertial stabilization systems in [24] which results a more robust controller under condition changes.

Moreover [33] experiments with another stewart platform with a force controller with effective results in isolation the disturbances between a range of 50 to 200Hz in addition a specially designed passive isolator.Fig. 2.9 illustrates the vertical transmission of the platform under disturbance with and without control. While the straight lines are the simulation results, dashed lines shows the experimental outputs of the system. A more complex control algorithm is presented on [27]. An adaptive disturbance cancellation methodology is used for the stewart platform during the study.

[42] deals with the forward and inverse kinematics of this system with a model-based PD controller. So ideally every disturbance could be rejected by using this system. Also [40] implements a robust auto disturbance rejection controller with the same platform and tested their controllers on disturbance and measurement noise with using a PD controller. Since many researchers implement advanced controllers [42]

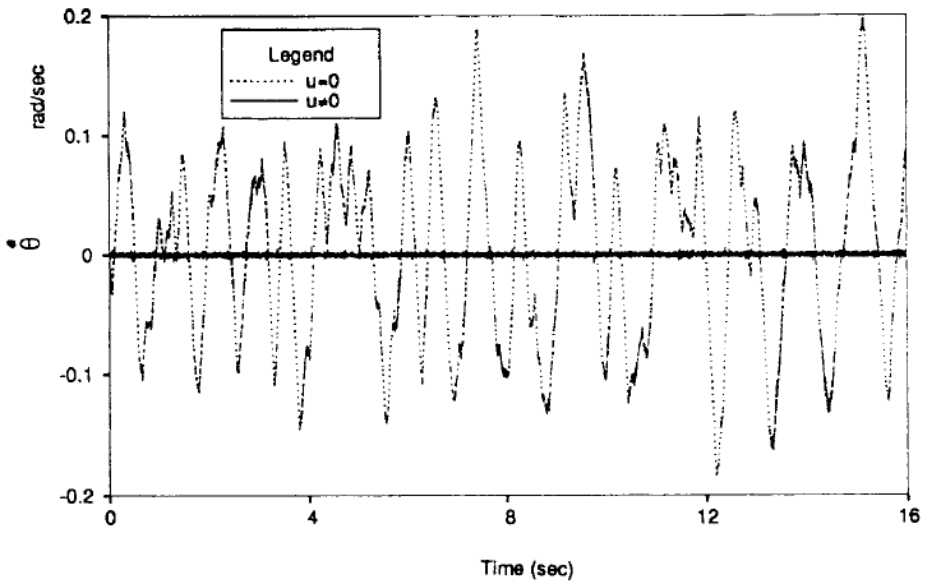

Figure 2.8: Comparison of LOS rate when control is and is not applied [25].

Table 2.1: Summary of the Performance Characteristics of Pendulum's Angle [30].

Specifications	LQR	PID
Settling Time	3.34 s	4.48 deg
Maximum Over Shoot	20 deg	0.5 deg
Steady State Error	0 deg	0 deg

and [40] shows the performance of traditional controllers. Tracking performance of sinusoidal signal by using a PD controller is resulted as Fig. 2.10. While tracking error of specific sinusoidal signal is given in right and the tracking signal is given in left.

Since our study gives a comparative evaluation of PID and LQR control for a head/camera platform. Similar comparetive studies are investigated. [6] talks about the advantages of fuzzy PID over traditional ones. And [9] compares LQR and a robust controller and shows the superiority of LQR controller in an inverted pendulum setup. A similar performance comparison of PID and LQR controller is done by [30] where results of this study is presented in Table 2.2 and Table 2.2. The results of both methodologies for controlling an inverted pendulum is presented by Nasir and his colleagues. Even though both controller are capable of stabilizing the inverted pendulum, the performance of LQR controller is proven to be better in Nasir's study. Those results gives us hints about the performance of both controllers in our systems.

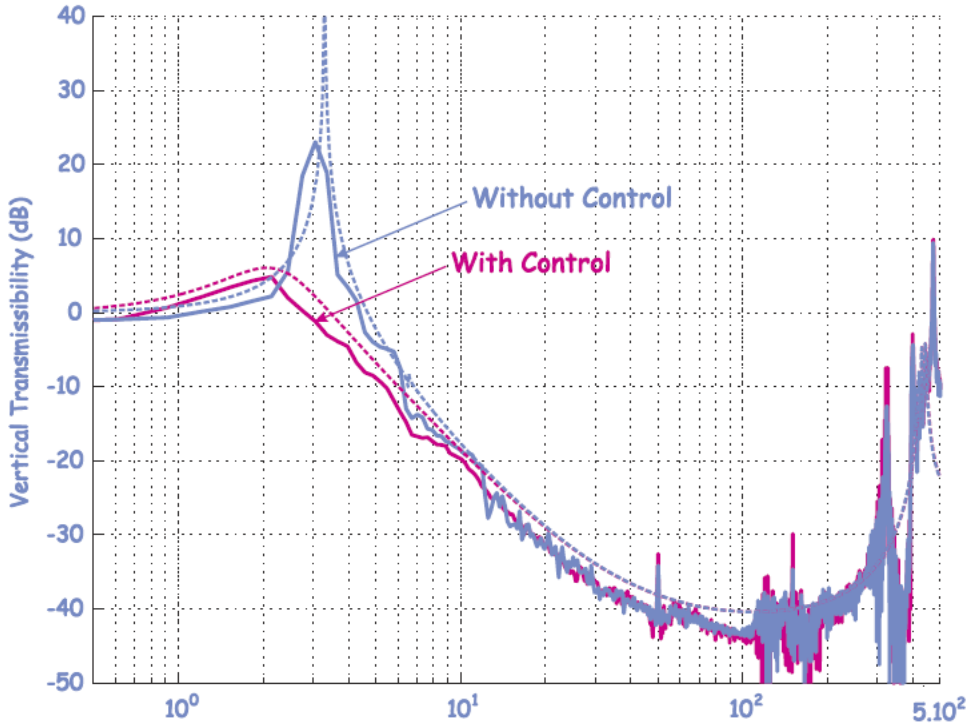

Figure 2.9: Configuration of 6-DOF Gough-Stewart Platform [42].

Table 2.2: Summary of the Performance Characteristics for the Cart's Position [30].

Specifications	LQR	PID
Rise Time	0.41 s	1.50 s
Settling Time	2.04 s	3.59s
Percent Overshoot	0.00	0.32
Steady State Error	0 cm	0 cm

Moreover at most of the applications servo systems are used. But in some light systems as hard disk drives [26] PZT-actuated suspension is also used. However in our application we have decided to use a linear DC motors and control it by using different approaches.

As a difference from above mentioned designed, our platform stabilization system will consist of three actuator and has a capability of 3 DOF motion. However the desired disturbance cancellation is in the roll,yaw and pitch axis in our robot SensoRHex. So the proposed design handles the problem occurred due to our robots motion.

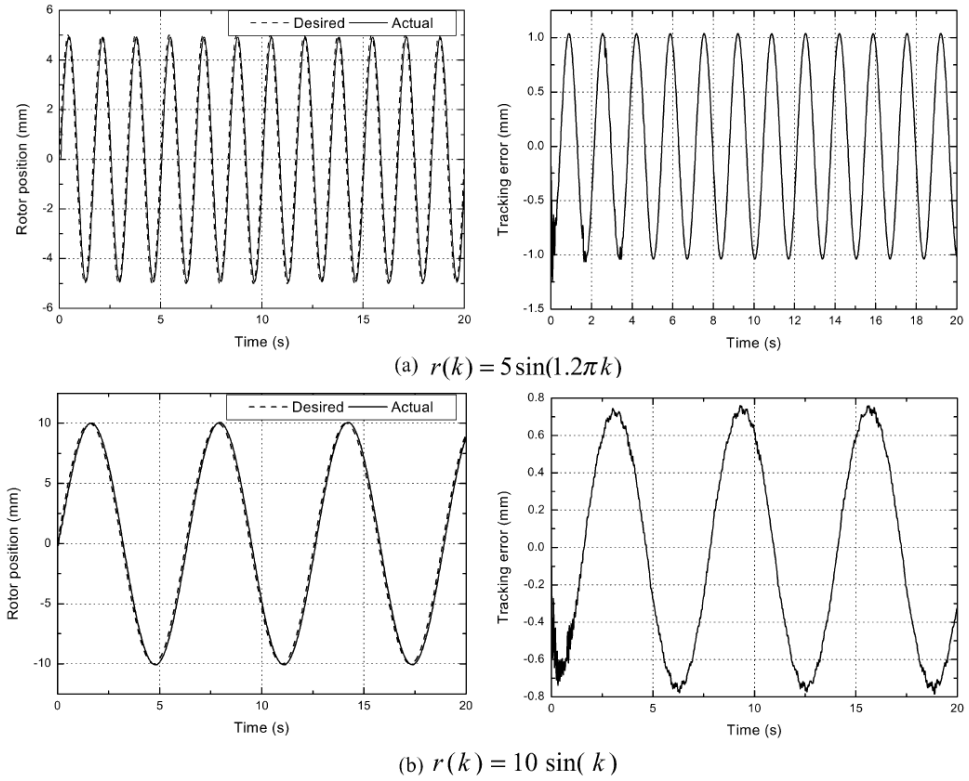

Figure 2.10: Configuration of 6-DOF Gough-Stewart Platform [42].

CHAPTER 3

THEORY

Since the main motivation behind this study is to design a robot head namely a camera stabilization platform on which a camera is mounted and has a capability of disturbance cancellation in all roll,yaw and pitch axis. However a planar head stabilization platform is designed in order to investigate the problem in a simpler architecture with the ability of disturbance cancellation only one axis. As a result, present study focuses on a stabilization platform which can only compensate the disturbances occurs on a single axis, for the six legged robot Rhex. Also in order to have more insight in PID and LQR controllers, a linear inverted pendulum which has a similar dynamic model with the head model, is controlled using those controllers. Due to availability and similarity of characteristics inverted pendulum model is selected. Moreover this study allows us to observe and compare the performances of those controllers with a system that has similar characteristics of the head model namely inverted pendulum and the head model. This chapter summarizes the theoretical background used during designing and controlling both the inverted pendulum and head stabilization platform.

3.1 Linear Actuated Planar Head Model

Main objective of this research is to implement a robot head that can reject the disturbances occurring due to the motion of our legged robot. During our experiments rotational movements in 3 axis, that could effect the performance of vision based algorithms, is observed. However as a start a one axis planar head model or in other words a planar head stabilization platform is designed to see and overcome the

difficulties of the main problem in a simpler architecture. This model Fig. 3.1 has the capability of stabilize rotational movements in one direction only with a linear DC motor.

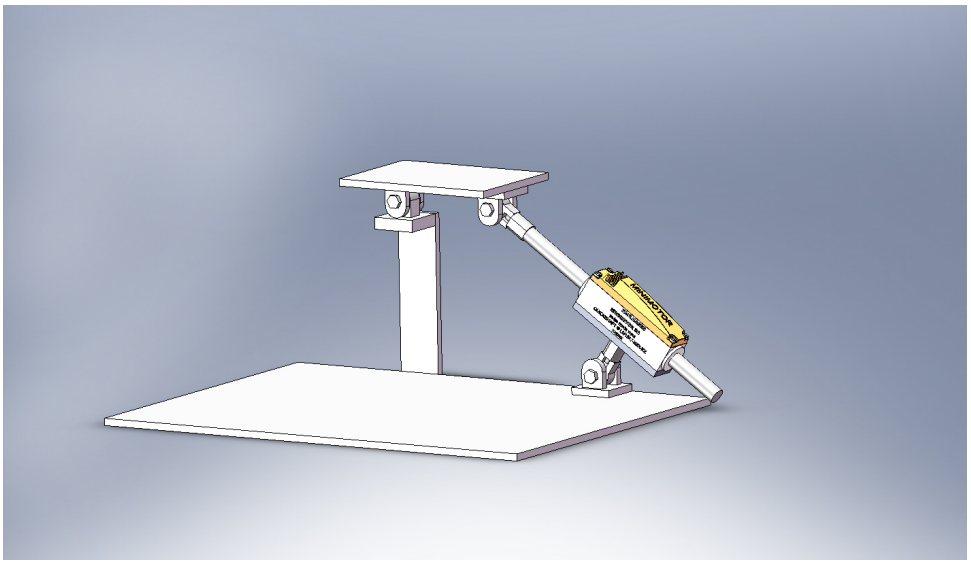

Figure 3.1: 3D Schematic of Linear Planar Head Model in Solidworks.

Mathematical model of the linear planar head model is carefully derived in order to create a realistic simulation environment. PID and LQR controllers are tested on this simulation platform as a start of the research on single axis head stabilization. However before starting to model the structure of head stabilization model, parameters of the system must be defined. Four main variables are used in order to determine the simulation model. θ represents the base platforms angle with respect to ground. ϕ is the camera platform angle with respect to Fig. 3.2 shows those parameters in the diagram of the head model.

3.1.1 Position Analysis

Before analyzing the system the correspondence of the parameters to the real world must be discussed. s is the length of the linear DC motors shaft. And it is the parameter that will be controlled by the control algorithm in order to obtain a stable head movement. More importantly ϕ which is the camera platform angle with respect to base platform is the parameter that is observed and measured. Moreover ϕ or $\dot{\phi}$ are

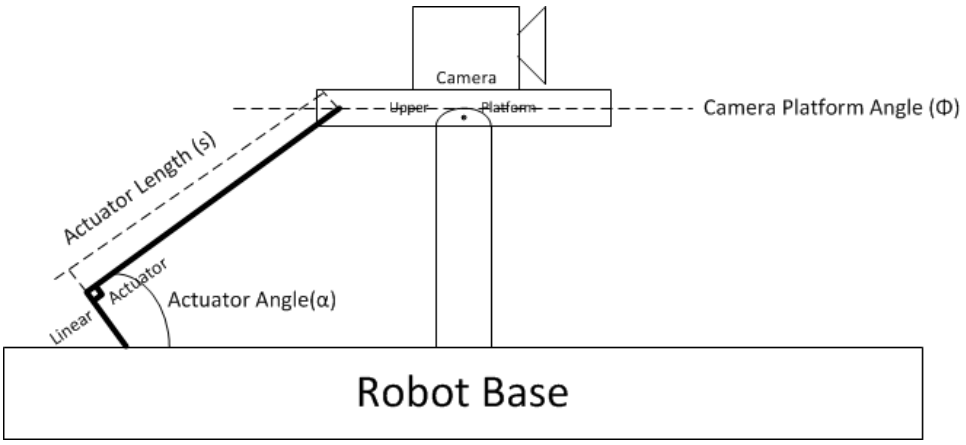

Figure 3.2: 2D Schematic of Linear Planar Head Model.

the system variables that will be stabilized by certain control algorithms. Three main position derivations are conducted in order to aid the force analysis of the system. As Fig. 3.2 illustrates, a is the height of the stabilization platform, where distance between the end of the actuator shaft and center of the camera platform is b and, d is the horizontal distance between the actuator joint and the center of the camera platform. c is the vertical distance between the actuator joint and actuator shaft. And s is the length of the actuator as discussed. Using complex plane approach in mechanism analysis following equations are derived.

$$se^{j\alpha} - be^{j(\pi-\phi)} = d + ja \tag{3.1}$$

$$se^{-j\alpha} - be^{j(\pi-\phi)} = d - ja \tag{3.2}$$

From (3.1) and (3.2), (3.3) is obtained.

$$s = f(\phi) = \sqrt{a^2 + b^2 + d^2 - c^2 + 2bdcos(\phi) + 2basin(\phi)} \tag{3.3}$$

Then by using trigonometric relations (3.4), (3.5) and (3.6), the required position analysis is obtained as (3.7) and (3.8).

$$Acos(\alpha) - Bsin(\alpha) = C = Rcos(\alpha + \gamma) \tag{3.4}$$

$$R^2 = A^2 + B^2 \tag{3.5}$$

$$\gamma = tan^{-1}(B/A) \tag{3.6}$$

$$\phi = g(s) = cos^{-1}\left(\frac{s^2 - a^2 - b^2 - d^2 + c^2}{\sqrt{(2bd)^2 + (2ba)^2}}\right) + tan^{-1}(\frac{a}{d}) \tag{3.7}$$

$$\alpha = h(s) = cos^{-1}\left(\frac{s^2 + a^2 - b^2 + d^2}{\sqrt{(2bd)^2 + (2ba)^2}}\right) + tan^{-1}(\frac{a}{d}) \tag{3.8}$$

However in force analysis (3.9) is required which is a derivation of the above analysis.

$$\alpha(t) = j(\phi(t)) \tag{3.9}$$

After obtaining above equations, speed and acceleration analysis must be done in order to complete force analysis for a realistic simulation environment.

3.1.2 Velocity And Acceleration Analysis

There exists two kinds of motion; rotational and translational. The motion kind must taken into consideration while conducting the velocity and acceleration calculations. However in our system there exist no translational motion. By studying the rotational motion of the system, velocity and acceleration vectors of ϕ and α is obtained. Velocity equations are obtained by Cramer's Rule by using position analysis.

$$w_\phi = \frac{js}{be^{j(\alpha-\phi)}} \tag{3.10}$$

$$w_\alpha = \frac{j\dot{s}b(e^{j(\phi-\alpha)} - e^{j(\alpha-\phi)})}{-2bse^{j(\alpha-\phi)}} \tag{3.11}$$

Moreover acceleration equations can be obtained easily by simply taking derivative of the (3.10) and (3.11).

$$a_\phi = \frac{dw_\phi}{dt} \tag{3.12}$$

$$a_\alpha = \frac{dw_\alpha}{dt} \tag{3.13}$$

By putting those analysis into force equations, a complete system analysis could be obtained.

3.1.3 Force Analysis

Force analysis is required in order to create a simulation environment. As seen in Fig. 3.3 force is applied to the camera platform from the linear actuator which is the control input of the system.

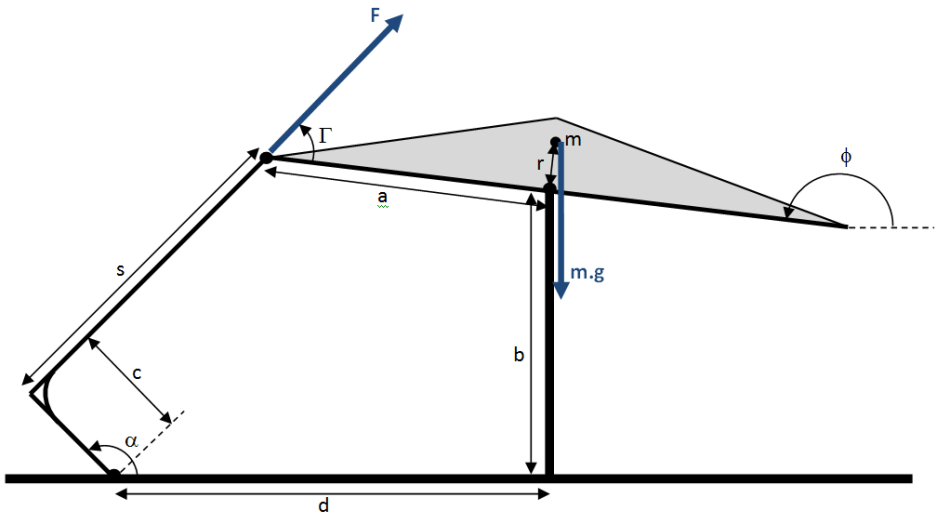

Figure 3.3: Diagram of the Planar Head Model.

As a start moments around a certain point and forces in three axis must be zero.

$$\sum M = 0 \tag{3.14}$$

$$\sum F_x = 0 \tag{3.15}$$

$$\sum F_y = 0 \tag{3.16}$$

$$\sum F_z = 0 \tag{3.17}$$

3.1.4 Non-linear State Space Model

The aim of this analysis is to find the $\ddot{\phi}$ as a state space variable.

$$\ddot{\phi}(t) = [m_{cam} g r sin(\phi(t)) - B_{head}\dot{\phi(t)} + F(t) a sin(\Gamma(t))] \frac{r}{m_{cam} r + I_{cam}} \tag{3.18}$$

$$\Gamma(t) = \alpha(t) + 90 - \phi(t) \tag{3.19}$$

$\Gamma(t)$ is the angle of force applied to the head stabilization platform and can be written in terms of α and ϕ as (3.19). Moreover, B_{head} is the viscous friction at the joint which connects the stabilization platform to the body of the robot. r is the distance between the center of mass of the camera and that joint and h is the distance between the end of the stabilization platform where the force is applied and the center joint.

In equation (3.18) by finding $\ddot{\phi}$ in terms of other variables state space of the system could be obtained where $\dot{\phi}$ and ϕ are the state space variables.

Moreover, in order to create a realistic simulation of the dynamic head stabilization platform, motor model must be added. Motor voltage will be the controller output in the real applications, so the relation between the applied force and the motor voltage must be derived and added to the model of the system. By adding (3.20) to (3.18) a more realistic simulation model is created. Where $V_m(t)$ is the motor voltage, K_t is the force constant and K_b is the back emf constant of the motor. Also note that motor inductance is neglected in this formula in order to create a fast working simulation model.

$$F(t) = \frac{V_m(t) - K_b\dot{s}}{R_a} K_t \tag{3.20}$$

3.1.5 Linearization of the Model

Although we have a non-linear system, linear controllers are investigated in this study. Moreover in order to implement a LQR controller linear state space model must be derived. Second order equations are linearized by using Jacobian linearization method to find state space matrices as similar to the inverted pendulum model.

$$\ddot{\phi}(t) = [m_{cam} g r \phi(t) - B_{head}\dot{\phi(t)} + F(t) a 0.7] \frac{r}{m_{cam} r + I_{cam}} \tag{3.21}$$

$$\dot{x(t)} = Ax(t) + Bu(t) \tag{3.22}$$

$$A = \begin{bmatrix} 0 & 1 \\ a_{21} & a_{22} \end{bmatrix} \tag{3.23}$$

$$x(t) = \begin{bmatrix} \phi \\ \dot{\phi} \end{bmatrix} \tag{3.24}$$

$$B = \begin{bmatrix} 0 \\ b_2 \end{bmatrix} \tag{3.25}$$

$$a_{21} = \frac{m_{cam} g r^2}{m_{cam} r + I_{cam}} \tag{3.26}$$

$$a_{22} = \frac{-B_{head} r}{m_{cam} r + I_{cam}} + \frac{K_b K_t b d}{R_a \sqrt{a^2 + b^2 + d^2 - c^2 + 2ba}} \tag{3.27}$$

$$b_2 = \frac{hr 0.798 K_t}{(m_{cam} r + I_{cam}) R_a} \tag{3.28}$$

After finding the linearized model of the system, control parameters for LQR control are obtained easily.

3.2 Background on Controller Models

As mentioned at the beginning of this document a linear inverted pendulum and a planar head model is controlled by using different control strategies and their performances are compared under different experimental scenarios. As a start, a brief introduction of controllers will be given.

3.2.1 Proportional Integral Derivative Controller

One of the most common controllers used in the literature is PID (Proportional-Integral-Derivative) controller. With its simple structure it is also one of the most general control algorithm that is used in the industry. Many instruments and engineers are using this method daily. Eventhough PID controller is not a new controller its effectiveness is still valid with comparison to other more developed and complex techniques.

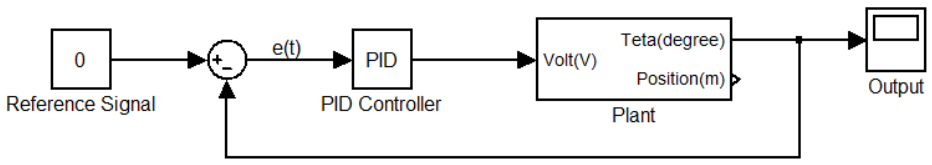

Figure 3.4: Block diagram of the PID controller in MATLAB Simulink Environment.

A basic representation of PID control is given in Fig. 3.4 PID control basicly takes the amount of error in the control parameters (angle in our case) and applies input to the system according to its parameters. K_P : position constant , K_D: derivative constant and K_I :integral constant are the three parameters of this control. Effects of increasing these parameters to the mains system response is given in Table 3.2.1.

Textbook version of PID control algorithm can be described as ;

Table 3.1: Effects of Increasing PID Control Parameters to the Performance of the System.

Response	Rise Time	Over-Shoot	Settling Time	S-S Error
K_P	Decrease	Increase	NT	Decrease
K_I	Decrease	Increase	Increase	Eliminates
K_D	NT	Decrease	Decrease	NT

$$u(t) = K_P e(t) + K_D \frac{de(t)}{dt} + K_I \int e(\Gamma) d\Gamma \tag{3.29}$$

3.2.1.1 Proportional Action

In the case of proportional control, equation simplifies to;

$$u(t) = K_P e(t) + u_b \tag{3.30}$$

In just proportional action, control action is directly proportional to the error of the controlled signal. Proportional action is the fundamental element of the PID control. Other actions are mainly effects the performance of proportional action.

3.2.1.2 Integral Action

Integral action ensures that the plant output agrees with the set point in steady state. Usually proportional action, leaves a steady-state error in the control signal. Integral action provides an increasing effect to the small errors, which changes the control signal no matter how small the error is. The equation of PI control can be given as ;

$$u(t) = K_P e(t) + K_I \int e(\Gamma) d\Gamma \tag{3.31}$$

Steady State error is removed when K_I has nonzero values. For small values of K_I the response of the system moves slowly towards the reference point. This approach is faster for larger values of K_I. However in this case response becomes more oscillatory.

3.2.1.3 Derivative Action

Derivative action improves to closed-loop stabilization performance of the controller. Because of the process dynamics, it will take some time for the controllers output become noticeable to a sudden change. So the response of the controller can not reach the speed of input change, this will result unstability. Derivative action in PD controller basicly, responds to the rate of change of the controlled state. The equation of PD controller can be given as;

$$u(t) = K_P e(t) + K_D \frac{de(t)}{dt} \tag{3.32}$$

3.2.1.4 Filtering the Derivative Action

Although derivative in PID control increases the system performance and response time significantly, there is a main trade off using this approach. Pure derivative action has very high gain for high frequency changes. Thus results large changes in the control output due to that noise. Eventhough the need for filtering in simulation environment is relatively small, in real experimenting a derivative control without the filter produces large amplitude noises which becomes the system uncontrollable.

3.2.2 Double Proportional Integral Derivative Controller (PID-PID)

One of the main drawbacks of PID controller is that it can only control one state of the system. However in our case our pendulum has two states to be controlled, angle and position of the pendulum. In order to overcome this problems two PID controllers are used, each of them controlling each state and their output are summed to be applied to the plant. Fig. 3.5 illustrates the block diagram of PID-PID controller

This controller creates a control signal which is the sum of two PID controllers. They individually create outputs with respect to error of angle of the pendulum and error of carts position. With the suitable parameters an effective control can be implemented. Although PID control algorithms like Zeigler Nicolas Method does not apply in this case with fine tunning of both parameters in controllers, successful results are obtained.

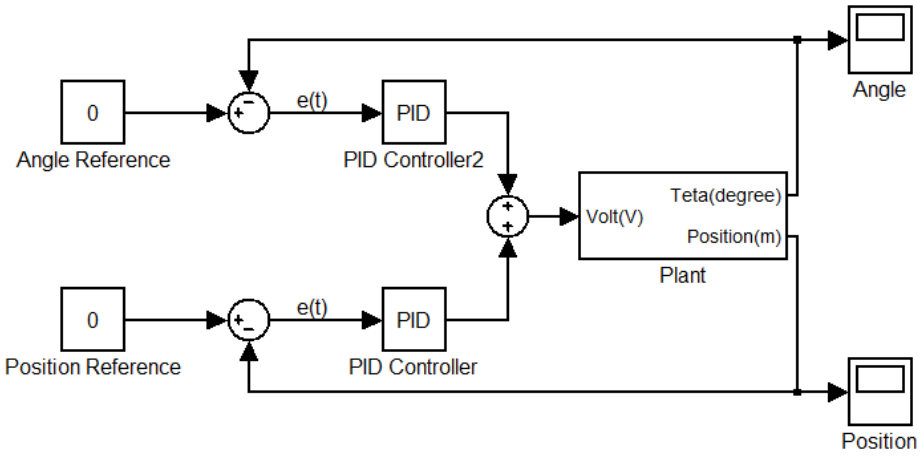

Figure 3.5: Block diagram of the PID-PID controller in MATLAB Simulink Environment.

3.2.3 Linear Quadratic Regulator Controller

The Linear Quadratic Regulator (LQR) is an optimal controller that requires a state-space linear approximation of the non-linear system but generally has superior performance. LQR measures all states and produces a plant input as a function.LQR stabilizes the system using full state feedback. Fig. 3.6 shows the schematic of the LQR controller.

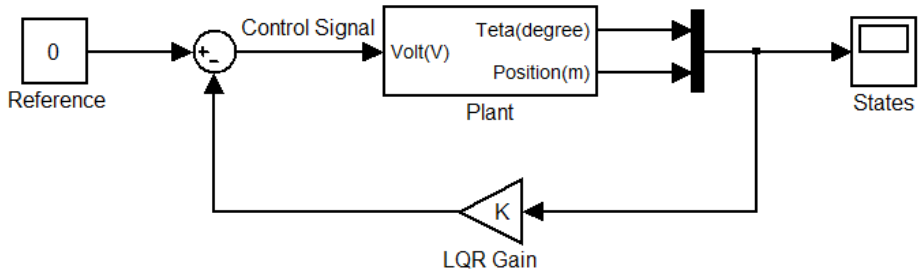

Figure 3.6: Block diagram of the LQR controller in MATLAB Simulink Environment.

Suppose that state space equations of linear time invariant system is ;

$$\dot{x(t)} = Ax(t) + Bu(t) \tag{3.33}$$

$$y(t) = Cx(t) + Du(t) \tag{3.34}$$

Performance index of the LQR controller is introduced as follows,where $u(t)$ is input and $x(t)$ is the state of the system.

$$J = 1/2 \int_0^\infty [x(t)Qx(t) + u(t)Ru(t)]\, dt \tag{3.35}$$

J must be minimal in order to achieve an optimal control. Q and R denote the weighting matrix of the state variable and input variable. An optimal control is dependent on Q and R matrix. However there is no common method in tuning those parameters. Usually simulation trial and error method is used for arranging the correct parameters. However note that in order to implement an optimal control an optimal control input must be found $u(t)$. (3.35) could be written as (3.36).

$$J = J_0 + 1/2 \int_0^\infty \left[(u(t) - u_0(t))' R(u(t) - u_0(t))\right] d(t) \tag{3.36}$$

Let P be a symmetric matrix, there exists such relation:

$$\int_0^\infty [x'(A'P + PA)x + 2x'PBu]dt = -x(0)'Px(0) \tag{3.37}$$

By adding and substrating (3.37) to (3.35), (3.38) is obtained.

$$J = x(0)'Px(0) + \int_0^\infty [x'(A'P + PA + Q)x + u'Ru + 2x'(PB + N)u]dt \tag{3.38}$$

Then the optimal control input which minimizes the cost function J is found as (3.39) by equating (3.36) and (3.38).

$$u_0 = -R^{-1}(B'P + N')x \tag{3.39}$$

Moreover Q and R have significant effect on the system performance, if R is large than a smaller input will be applied to stabilize the system. Also if the error in a certain

state needs to be small, the corresponding column of Q needs to be larger. Also keeping Q fixed and reducing R; results a decrease in transition time and maximum overshoot and an increase in rise time and steady state error.

$$u(t) = -Kx(t) \tag{3.40}$$

$$K = R^{-}1(B'P + N') \tag{3.41}$$

The optimal control input is also be found by the help of MATLAB function K = lqr(A,B,Q,R) where K is the LQR gain of the controller. Where the input is represented as (3.40).

By increasing the relative weight of the state 1 error gain $Q(1,1)$, the relative importance, in the cost function, of the state 1 error is increased and therefore tends to be minimized more effectively by LQR. This results better tracking in desired state 1.

By increasing the relative weight of the state 2 error gain $Q(2,2)$, the relative importance, in the cost function, of the state 2 error is increased and tends to be minimized more effectively by LQR. This results better regulation around zero of the state 2 .

By increasing the relative weight of the control effort factor $R(1,1)$, the cost of applying an input increases, there control effort spent will be reduced. For example, if the motor voltage comes into saturation, $R(1,1)$ needs to be increased or $Q(1,1)$ or $Q(2,2)$ reduced in order to decrease the input magnitude.

3.3 Passive Vibration Isolation

Eliminating the effects of external or internal disturbances is the main aim of the vibration isolation systems. Several approaches are developed on this field through several years since the wide application area of the subject. Vibration isolation systems are used in basically every kind of vehicles. For example: cars uses them in suspension systems, crucial electronics system of planes are protected by vibration isolators. Moreover a wide range of electromechanical systems like gimbals, stabiliza-

tion platforms, CNC machines uses isolators in order to decrease the vibration acts on those systems.

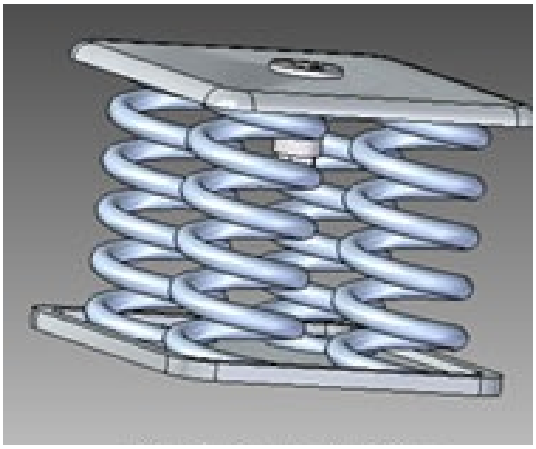

Figure 3.7: Passive Isolation of a Base Platform with Springs [5]

Passive and active vibration isolation are two main approaches to the problem. Passive vibration isolation is achieved by using structures like springs and dampers or shock mounts which consumes no external energy. Fig. 3.7 is an example of passive isolators. On the other hand, active vibration isolation systems uses energy to reject the disturbances acts on the system. Fig. 3.8 is a six degree of freedom active vibration isolation table which has four linear actuators in the legs of the table. A controller gives actuation commands to the legs of the table so that it remains horizontal position.

In our study passive isolation will be obtained by using elastomeric vibration isolators and a head stabilization platform powered by faulhaber's linear DC motors will succeed the active isolation.

Elastomers are rubber-like materials that deforms to absorb mechanical energy. Automobile engines, aircraft components, industrial machinery, and building foundations used elastomeric isolators for shock and vibration isolation. Since the rubber structure does show different characteristics under different directions, elastomers are better in one axis in the sense of isolation. Due to this characteristics four isolators will be placed at the bottom of the head stabilization platform like Fig. 3.9.

Before installing isolators to the systems the effects of isolation to the system must

Figure 3.8: Active Isolation with Actuation at the Legs of the Table [3].

be discussed. Behavior of the system changes by adding isolators to the system. And some constraints merge in order to obtain a stable and effective isolator. Any acting force or moment on the isolator creates linear or angular displacements which could cause dynamic coupling in the system and creates undesired movement of the body. Also natural frequency of the isolators and the body must be taken into consideration while designing an isolation platform. As close as the natural frequencies get the chance of dynamic coupling increases.

Dynamic coupling is not desired in stabilization platform. If a system has dynamic coupling a disturbance is not rejected effectively and also it will create rotary motions. So the followings must be conditions must be satisfied in order to reduce the dynamic coupling in the system:

-Isolators must be located on the same plane.
-Center of gravity of the load must be close to the mounting plate of isolators.
-Elastic axes of the isolators must be parallel to the coordinated axis of the system.
-Isolators kinds and locations must be selected in a manner that, stiffness constant must be proportional to the weight that acts on the system.

By taking those into consideration a passive isolation integration like Fig. 3.9 is merged. In order to analyze the system stiffness constant and natural frequency of

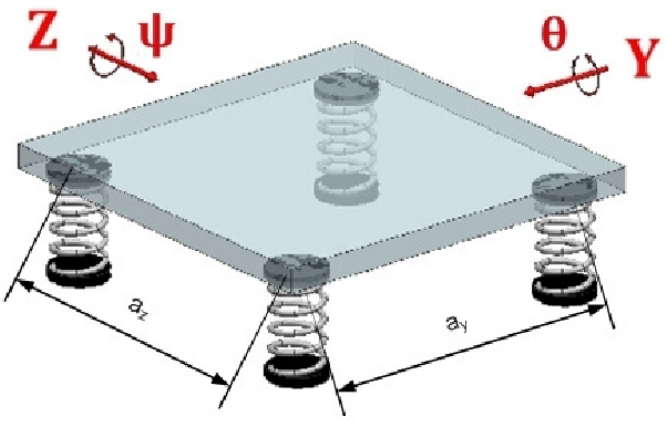

Figure 3.9: Passive Isolation with four Isolators Located at the Corners of the Platform.

the system must be found. As shown of the figure, plate has the ability to rotate in y and z directions. So both stiffness constants $K_t\theta$ and $K_t\varphi$ must be found in terms of spring constant and dimensions of the plate.

$$K_t\theta = ka_z^2 \tag{3.42}$$

$$K_t\varphi = ka_y^2 \tag{3.43}$$

Morely, rotary natural frequencies must be found by noting I_y and I_z are moment of inertias of the system around that axes.

$$w_n\theta = \sqrt{k/I_y}a_z \tag{3.44}$$

$$w_n\varphi = \sqrt{k/I_z}a_y \tag{3.45}$$

By adjusting those parameters a suitable passive vibration isolation platform can be obtained.

In order to determine the desired natural frequency and damping ratio of the passive

isolator for our system, several experiments are done with a high speed accelerometer which has a 10 kHz bandwidth. However there exists a mounted IMU (MicroStarin 3DM-GX1) on the RHex, but it has a bandwidth of 300Hz. So vibrations above this frequency can not be measured by this inertial measurement unit. So by using a high speed single axis accelerometer(Dytran 3035B) and its analyzer (HP3560 Dynamic Signal Analyzer) the vibrations acting on the robots body is obtained. Fig. 3.10 illustrates the vibrations on the system in terms of g force during walking at different speeds.

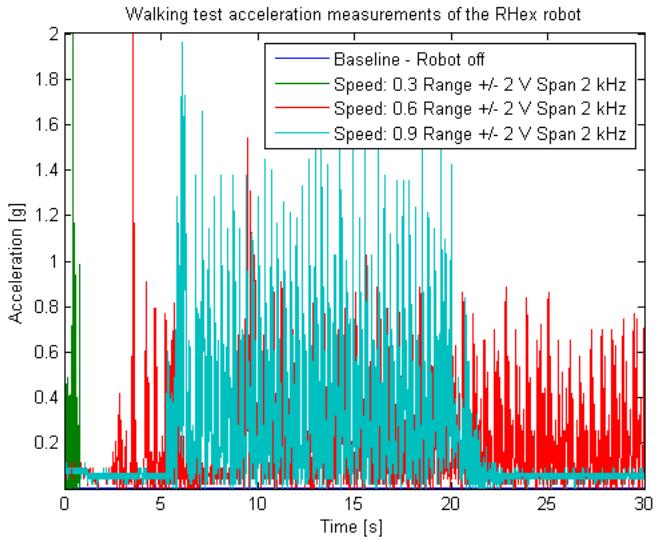

Figure 3.10: Acceleration Measurements taken by Dytran 3035B from the RHex Robot During Locomotion in Time Domain

A frequency domain analysis is useful during these situations, since one can understand the frequency values of the signal more clearly. Fig. 3.11 clearly indicates the signal in frequency domain. From figure it is clear that around 200Hz and 1000Hz there exists high frequency oscillations in the system due to the both motion and structural integrity of the Rhex. The vibrations in this range must be filtered out from the system by using a passive isolator.

However passive isolators do not have exact same characteristics as ideal low pass filters. The mathematical model of a passive isolator is shown in (3.46) where w_n is the natural frequency and ξ is the damping ratio of the isolator.

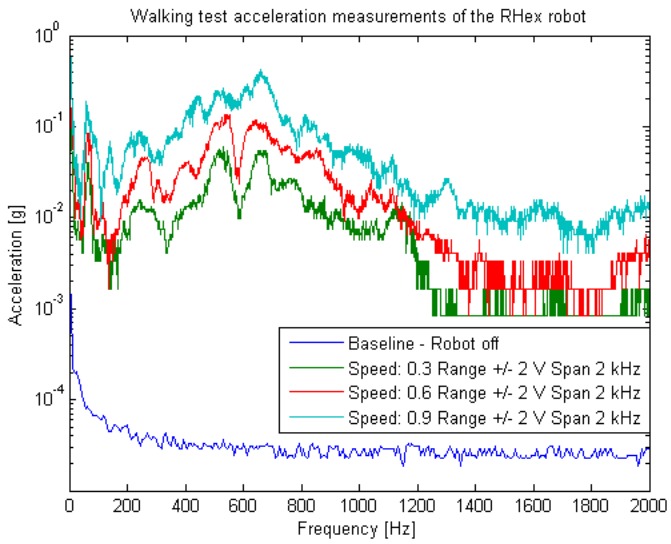

Figure 3.11: Acceleration Measurements taken by Dytran 3035B from the RHex Robot During Locomotion in Frequency Domain

Robot Speed	Max	RMS
0.3	0.6 g	0.00041 g
0.6	1.0 g	0.00098 g
0.9	1.9 g	0.00260 g

Table 3.2: Linear Acceleration with Different Robot Speeds.

$$H(s) = \frac{2s\xi w_n + w_n^2}{s^2 + 2s\xi w_n + w_n^2} \tag{3.46}$$

Bode plot of a typical passive isolation filter is shown in Fig. 3.12. While w_n selection effects the cutoff frequency of the filter, xi changes the filter reponse as seen in Fig. 3.12. With an incorrect damping ratio selection the frequency which is desired to be filtered out, can be amplified instead since with lower damping ratio gain of the filter increases above unity in a certain location.

As explained, robots body movements during legged locomotion is measured by using sensors at different robot speeds. And those movements are tried to be canceled out by using a head stabilization platform. However the high frequency disturbances in the robot body is elliminated by using a passive vibration isolator. Fig. 3.13 shows the results of the robot body motions with and without a passive isolator in FFT. It is clear that passive vibration isolator works as predicted and residual high frequency

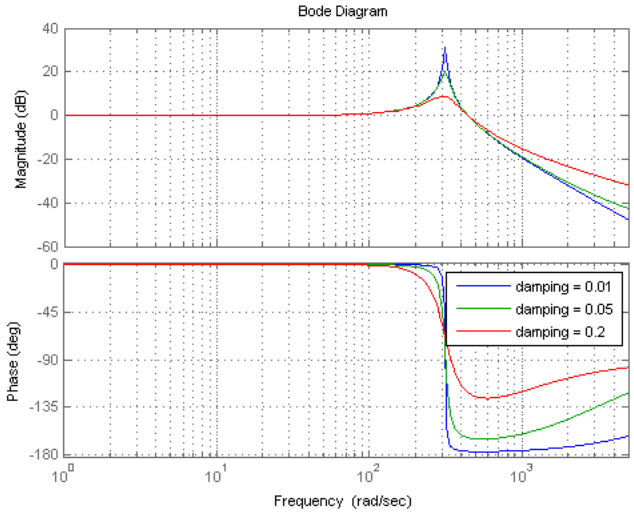

Figure 3.12: Bode Plot of Passive Isolation Filter with Different Damping Ratios

disturbances are much lower.

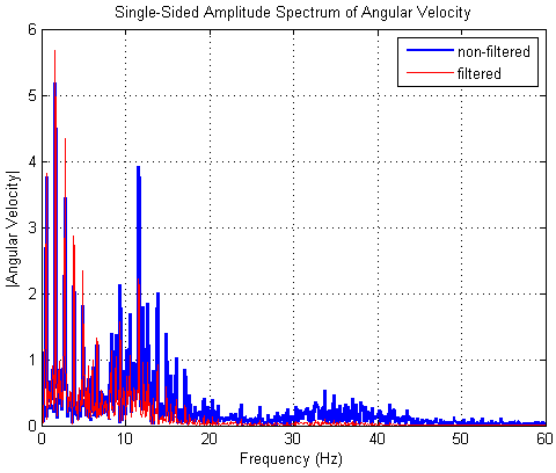

Figure 3.13: Passive Isolation with four Isolators Located at the Corners of the Platform.

CHAPTER 4

EXPERIMENTAL SETUP

In order to prove the concepts that are been discussed, characteristics of controllers with different models are be tested. Proposed controllers, PID and LQR are applied to a planar inverted pendulum and the head stabilization model.

This chapter includes the details of the proposed software and hardware design. Firstly mathematical models of those platforms are simulated on MATLAB by using simulink. Then hardware setups are mentioned in detail.

4.1 Introduction

Eventhough main purpose of this paper is to implement and compare both PID and LQR controllers in the head stabilization platform, similarities of head model and planar inverted pendulum encourages us to try the proposed algorithms firstly in planar inverted pendulum. There are several motivations behind this action.

As a start inverted pendulum in production sense, pendulum is more straight forward compared to a head stabilization platform. So by producing and obtaining and inverted pendulum setup, we can convert our theoretical discussions into a real world application with a convenient hardware. Also a precisely manufactured inverted pendulum setup is purchased from Quanser Company in Canada for a new student laboratory in Electrics and Electronics Department in METU. And theoretical ideas are also tested on that platform. Moreover in order to produce an effective head stabilization platform, many different ideas are discussed. As discussed in Chapter 2 part of the thesis, several ideas about this topic suggests a gimbal mechanism like Fig. 4.1

to overcome this problem.

Figure 4.1: A Typical Three Axis Gimbal Mechanism Used in Camera Stabilization[4].

After some series of discussion and many researches about this problem, idea of a stewart-platform like head stabilization platform merges. However in classical stewart platform there are six actuators to control the base platform. But in our case 3 small linear DC motors will power the platform in order to have to ability of yaw,roll and pitch movement. Because of the complexity of this three axis stabilization platform, a basic one axis stabilization platform Fig. 3.2, which has one actuator and capable of stabilizing only one axis, is studied as a start for the study. The experience gained from the planar head stabilization platform will guide the final research on the three axis platform which will have a design like Fig. 4.2.

4.2 Linear Actuated Planar Head Model

Eventhough inverted pendulum system is investigated first due to the similarities of head stabilization platform, purpose of the study is to design a head stabilization platform that can reject disturbances caused by our six-legged robot Rhex in order to reduce motion blur and aid other image processing algorithms. Those disturbances will have all; yaw,pitch and roll nature, but as a start one axis head stabilization platform is designed and anaylzed before carrying on the research in three axis disturbance rejection.

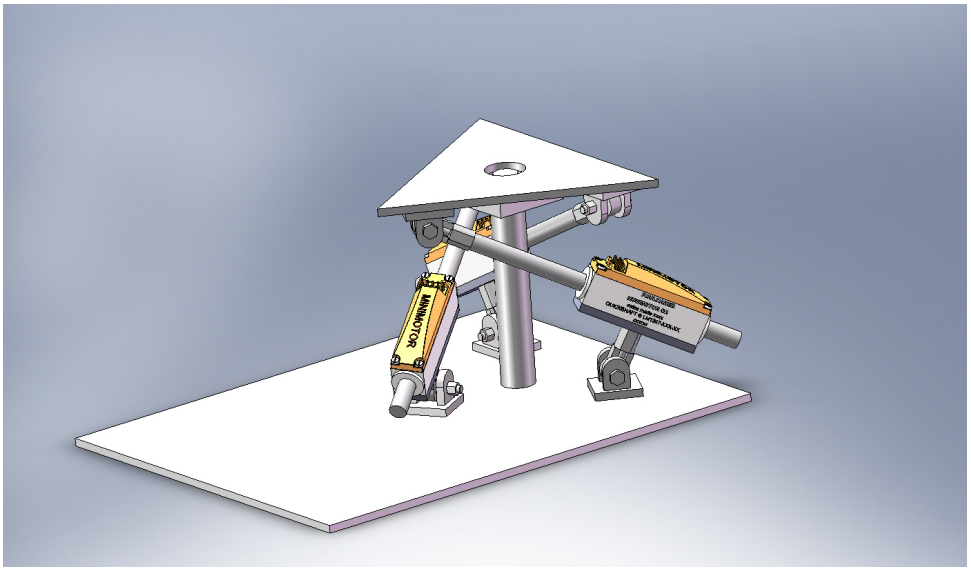

Figure 4.2: Three Axis Head Stabilization Platform designed for Rhex in Solidworks.

4.2.1 Simulation Model

As a start simulation the model is created by using MATLAB simulink from the calculations in Chapter 3. The state space model is used in order to implement the simulation model. In this model system input is the force applied to the camera stabilization platform and outputs are the ϕ and rate of change of ϕ. However while creating the plant model s is also given as an output for the use of motor model. Schematic of the head simulation model is given in Fig. 4.3. Voltage is applied to the motor as an input from the controller and motor gives force as an output which is used as an input to the head model.

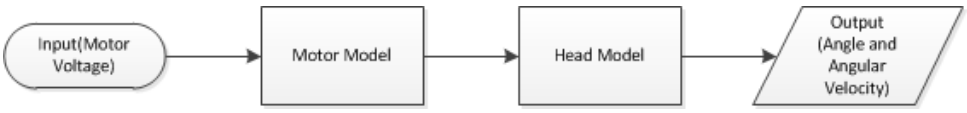

Figure 4.3: Simulation of Head Model.

The simulink model of the system is shown in Fig. 4.4. Main difference between traditional dc motored system is the usage of linear dc motor. In traditional DC motor modeling back Emf is caused by the angular movement of the rotor of the motor. However in our case there only exists translational motion. Therefore back emf is caused by the linear velocity of the motor shaft as seen in Fig. 4.4.

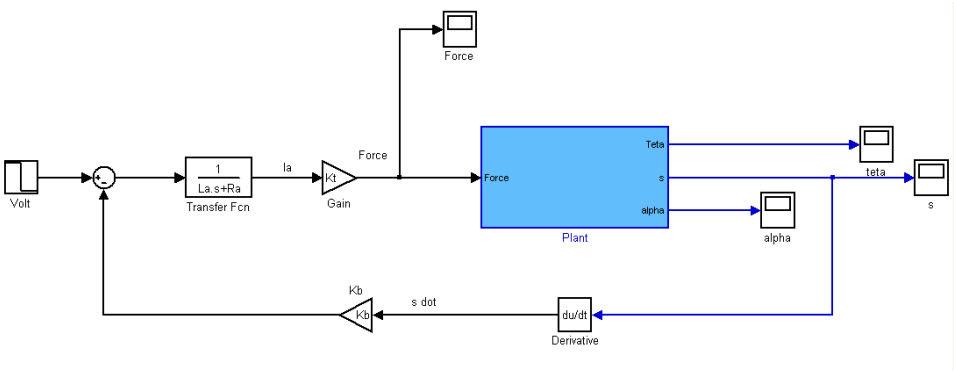

Figure 4.4: Flowchart of the Head Model Stabilization Model.

4.2.2 Actual Setup

The actual one-axis camera stabilization platform will like Fig. 4.5. Camera will be mounted at the top of the platform while the base will be fixed to the robot base. Linear motor can rotate the camera platform around at the center of it by applying force to the edge of the platform.

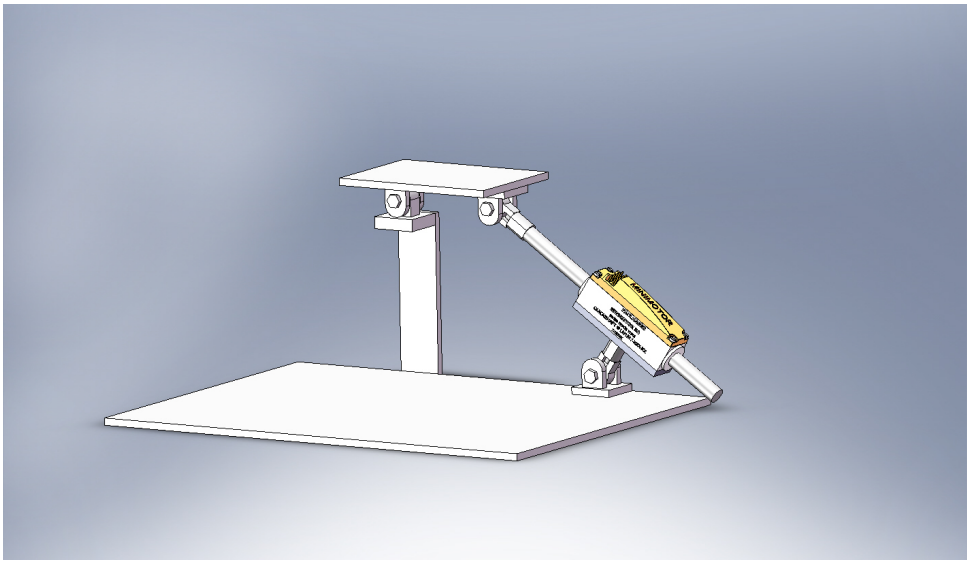

Figure 4.5: 3D Schematic of Linear Planar Head Model.

Motors are linear DC motors that are bought from faulhaber, also motor controllers are selected for this motor which will give us the ability to position and speed control as extra features. During simulations the actual motor parameters of faulhaber motors are used while performance of the system is being tested. And a detailed performance

comparison is given with using different motors.

4.3 Performance Measures

Different experiments are conducted in order to compare the performances of controllers in head stabilization setup. Step responses of the head/camera stabilization platform for the angular velocity is investigated. Comparison is done in the scope of rise-time, maximum overshoot , settling time and steady state error. Also sinusoidal tracking ability of the system is investigated and the specific signal tracking, which is taken from the real life experiments of robot SensoRHex by using an inertial measurement unit, during locomotion is given as a reference signal.

Also head model is studied and comparison of PID and LQR controller is done in the scope of performance measures. Moreover, a comparative tracking ability of head model is tested by using real experimental signals as a reference.

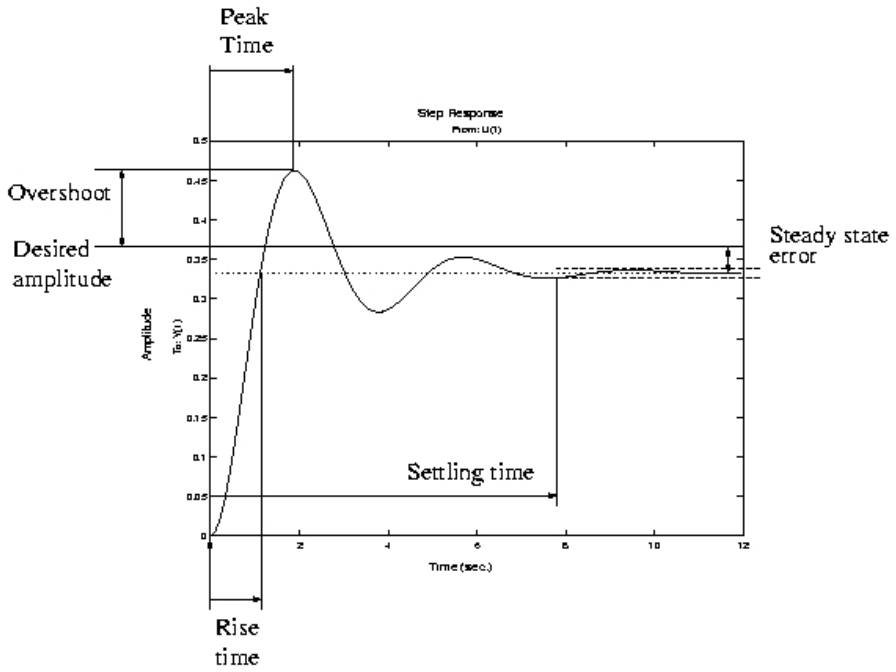

Figure 4.6: Graphic Illustration of Performance Measures.

CHAPTER 5

COMPARATIVE EXPERIMENTS WITH HEAD MODEL

In the scope of those teorical data a planar head stabilization model is designed and controlled with using two different control algorithms. And in different experimental scenarios a comparative evaluation of those control structures in a head stabilization platform is discussed. By using the model of the designed platform Fig. 5.1, different responses of the system is investigated by using PID and LQR control.

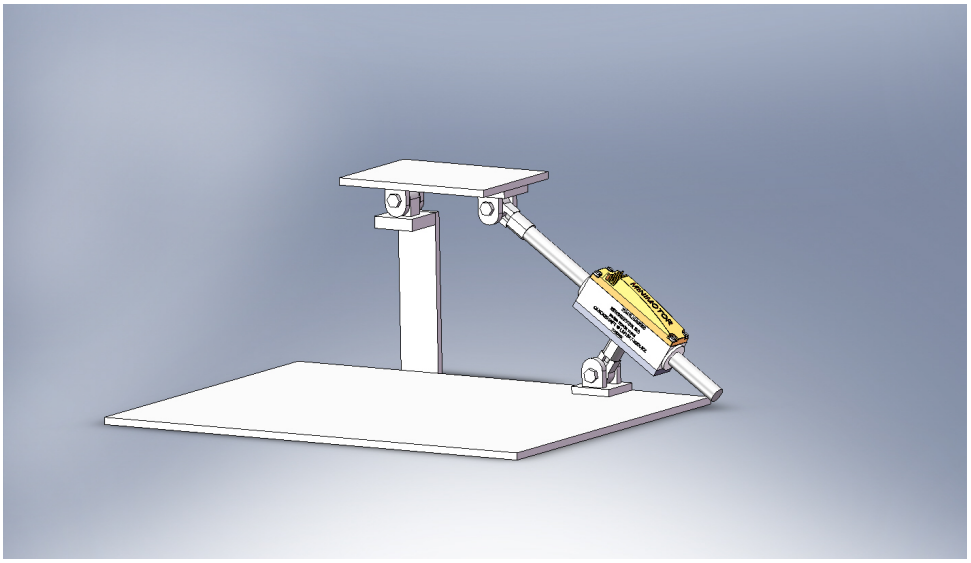

Figure 5.1: Illustration of Linear Planar Head Model Designed in SolidWorks.

The main motivation at the beginning of the study is to reduce the amount of motion blur on the image data taken from the robot, which occurs due to the rotational velocity of SensoRHex. Reducing the motion blur will increase the performance of image

processing algorithms. A head stabilization platform which controls and stabilizes the angular velocity is designed for this task. However also angular position of the stabilization platform could be taken under control but with a less weight.

After obtaining the step response of the system, tracking ability of the system is tested by applying first a sinusoidal signal as a reference and than the real experimental data obtained from an inertial measurement sensor mounted on the robot during locomotion.

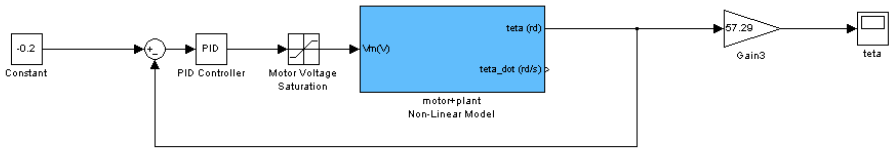

Figure 5.2: PID Control Block Diagram with Head Stabilization Model in MATLAB.

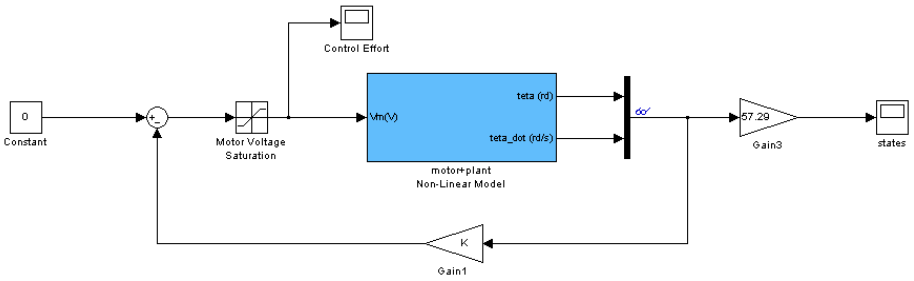

Figure 5.3: LQR Control Block Diagram with Head Stabilization Model in MATLAB.

Fig. 5.2 and Fig. 5.3 illustrates the control block diagrams of the head model with PID and LQR control sequentially in MATLAB Simulink environment. By using those control structures, a comparative evaluation of PID and LQR controllers in real life experimental conditions, is conducted in different experimental conditions.

5.1 Response to an Initial Non-Zero Angular Velocity

Before analyzing the system response with more realistic signals, the step response of the system to a non-zero initial angular velocity is obtained with two different controllers. Also their performances are compared in terms of performance measures.

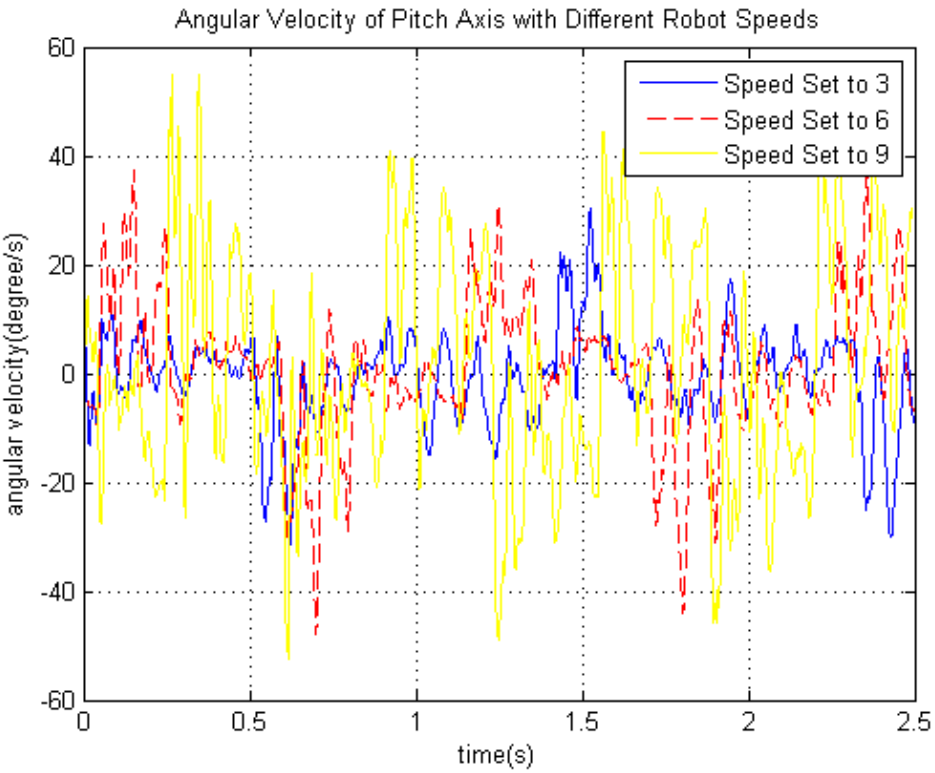

Figure 5.4: Non Filtered Angular Velocity of Pitch Axis with Different Robot Speeds

With different initial angular velocities different experiments are done and controllers effects on stabilizing the system is obtained. Since we are planning to stabilize movements of the robot base due to locomotion, the step response of certain angular velocity is investigated in the scope of the measurements taken from the experiments on SensoRHex. While experimenting during the measurement of the angular velocity and acceleration, the maximum amount of change in the angular velocity is decided as $120 degree/s$ as seen from Fig. 5.4. And simulations are conducted at the light of this data, three different results are obtained with initial non-zero velocities $60 degree/s$, $90 degree/s$ and $120 degree/s$ which are similar to the maximum amount of angular velocity change during three different experiments at different robot speeds.

Fig. 5.5 and Fig. 5.6 shows the angular step response of PID and LQR controller separately. Although LQR is a state space controller capable of controlling multiple states, weight of angular position is selected to zero in order to make an accurate comparison with the performance of PID control which only controls the system by the error in the angular velocity of the head model. It is clear that while angular

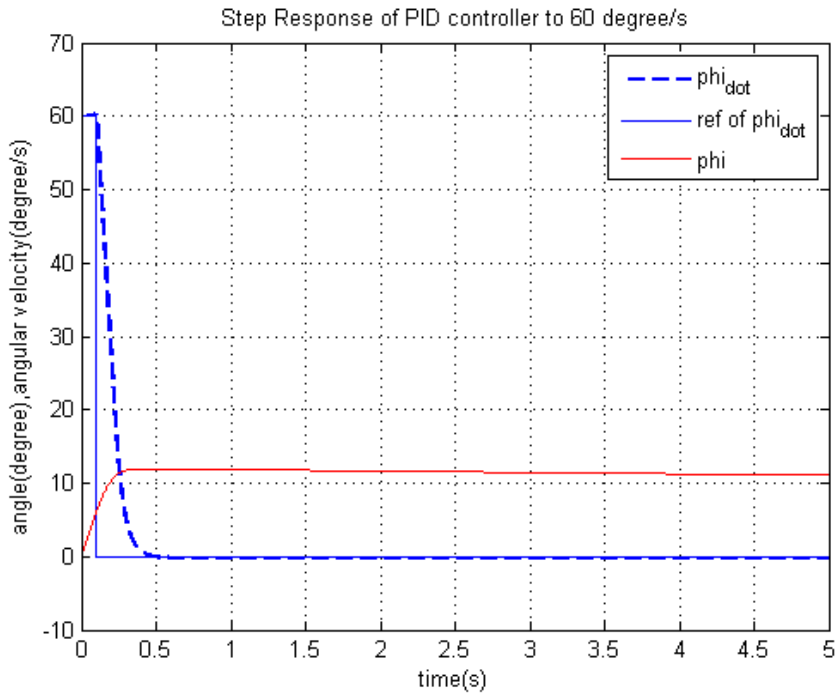

Figure 5.5: PID Control Step Response with a reference signal 60 degree/s.

velocity is setting to zero by the controllers, the angle of the head model remains constant.

However Fig. 5.7 is the response of the head model with LQR controller which has a 1/10 weight ratio of the states. This means that LQR controller tries to sets also the angle of the head model to zero while trying to balance the angular velocity. From Fig. 5.7 clearly illustrates this effect. Although by this approach, one can control over both states of the system, stabilizing performance of angular velocity is decreased as compared to Fig. 5.5 and Fig. 5.6.

In addition Fig. 5.8 and Fig. 5.9 are the step response of the system while angular velocity is set to 90 and 120 degrees/s which corresponds to the maximum amount of angular velocity change in the body of the Rhex with different experiments. Table 5.1 is prepared using the data in Fig. 5.5 and Fig. 5.6. In addition Table 5.1 uses data in Fig. 5.8.

However there is one crucial situation that can lock the system totally, and the force applied become obsolete. In a certain angle the force applied to the system will be

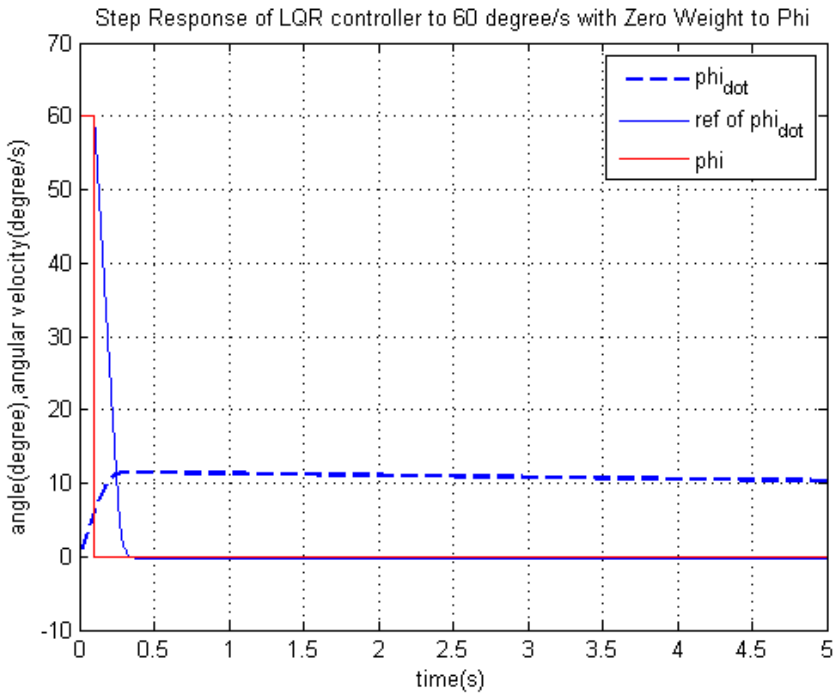

Figure 5.6: LQR Control Step Response with a reference signal 60 degree/s.

Table 5.1: Comparison of Angular Velocity Step Response of Controllers in 60deg/s as a Initial Condition.

Controller	Rt	Over-Shoot	St	S-S
PID	0.395 s	0 deg/s	0.636 s	0 deg/s
LQR	0.395 s	0 deg/s	0.636 s	0 deg/s

directed to the center of the shaft and this will results zero rotational force around that axis. Thus, effect of the actuator to the system become almost negligible. So limits of the control algorithm arises from this constraint. From geometric calculation the interval for the angle is found as +25 and -155 or to be more realistic, +25 -25 degrees could be considered as the limit of the system, above this range controller will fail due to geometric constraints.

However, although the proposed algorithm seems to be sufficient for this problem, it has drawbacks in terms of stabilizing the angle of the platform. So during the stabilization of the actual head stabilization platform angle of the platform must also be controlled with a lower weight with respect to the angular velocity.

Tunning of both controllers are one intuitively, since the effects of all the parameters

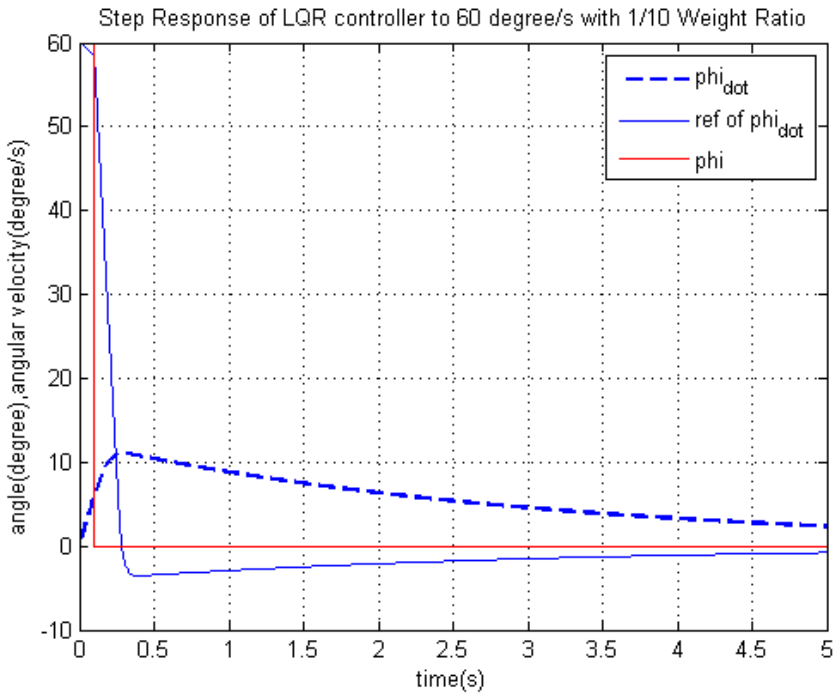

Figure 5.7: LQR Control Step Response with a reference signal 60 degree/s with a 1/10 Weight Ratio.

Table 5.2: Comparison of Angular Velocity Step Response of Controllers in 90 deg/s as a Initial Condition.

Controller	Rt	Over-Shoot	St	S-S
PID	0.395 s	0 deg/s	0.487 s	0.5 deg/s
LQR	0.395 s	0 deg/s	0.446 s	0.5 deg/s

are known to the controller performance fine tuning is achieved. However as an initial step for PID controller Zeigler-Nicolas method is used in order to obtain the rough PID parameters and for LQR control a special MATLAB function is used in order to obtain the optimized gain for the controller and by using trial and error method suitable Q and R parameters are selected.

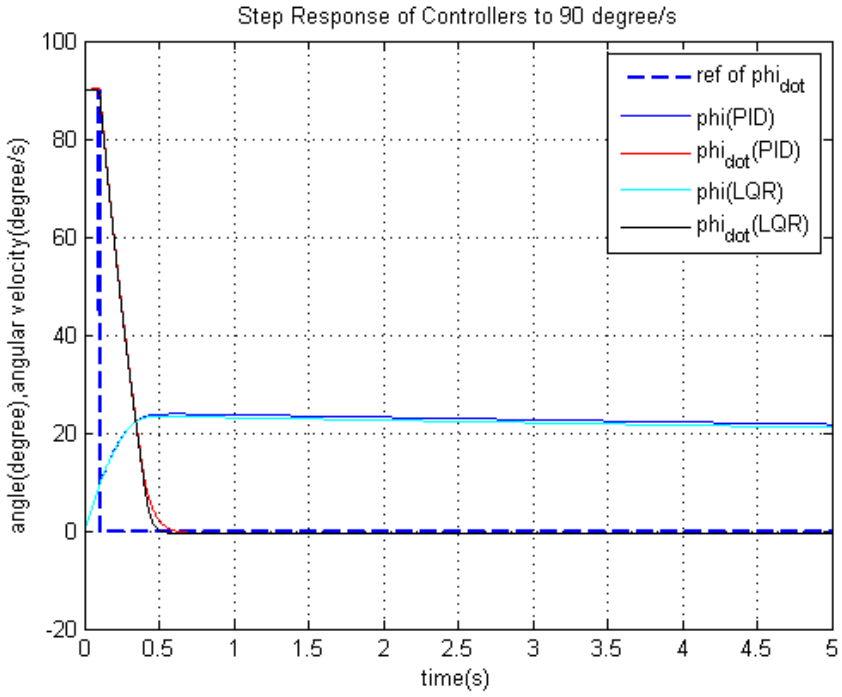

Figure 5.8: Controllers Step Response with a reference signal 90 degree/s.

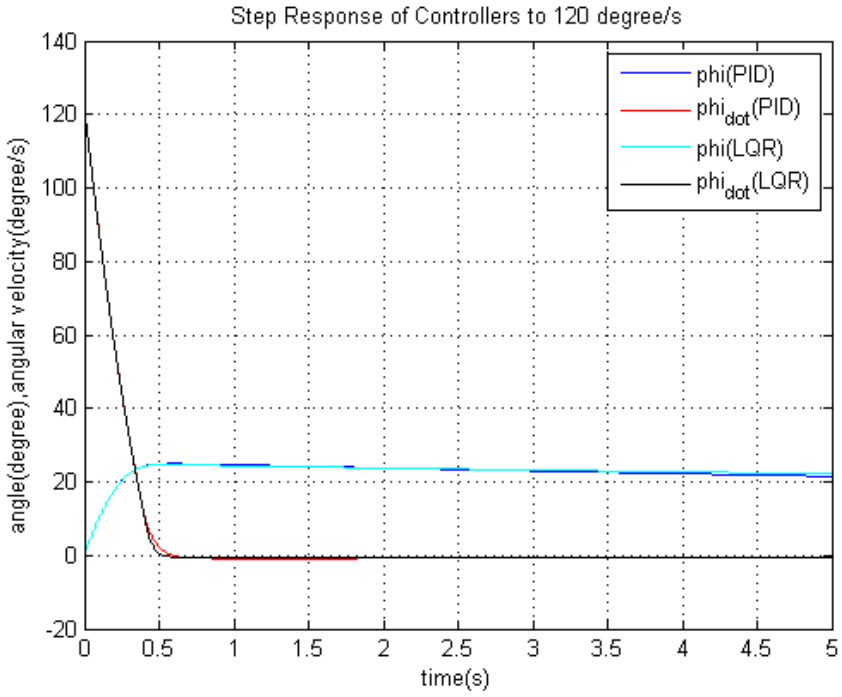

Figure 5.9: Controllers Step Response with a reference signal 120 degree/s.

5.2 Tracking Sinusoidal Signal

Before testing the system with the actual experimental data, sinusoidal signals with the similar amplitude and frequency as the experiments which are done at three different velocities of our robot SensoRHex is tested as a tracking reference. Investigating the performance of the controllers with a virtual $\dot{\phi}$ signal will gives clues about the characteristic behavior of our system under oscillations occurs in the robots body. Amplitudes and frequencies of those signals are be decided by investigating experimental data and illustrated in Table 5.3. Since the main parameter that is aimed to be controlled is the angular velocity, two different approaches are tried in stabilizing the oscillations in angular velocity.

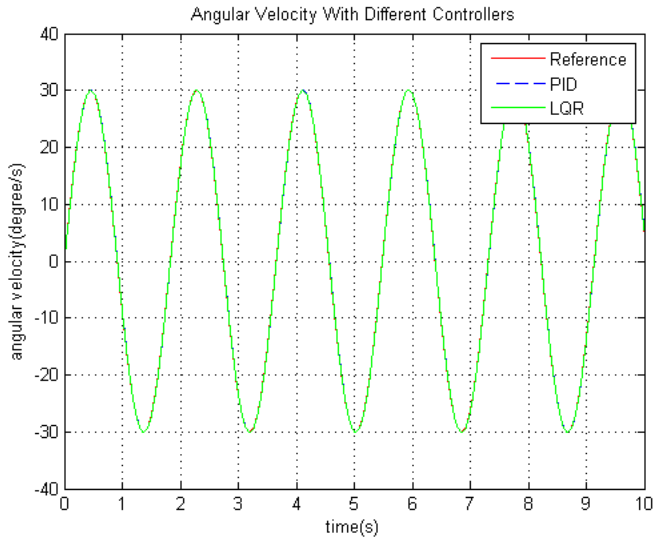

Figure 5.10: Tracking of Sinusoidal Signal with an Amplitude of 30 deg/s which Corresponds to the Maximum Angular Velocity Change of Rhex Signal with Robot Speed Set to 0.3.

Angular velocity is selected as a reference and tracking ability of controller by using $\dot{\phi}$ as a reference is discussed. Fig. 5.10 and Fig. 5.12 shows the tracking performance of PID and LQR controller when a sinusoidal signal is applied which represents the SensoRHex experiment with speed set to 0.3 and 0.6. Also the error in tracking the sinusoidal reference is shown in Fig. 5.11 and Fig. 5.13 it is clear that residual oscillations in the robot body remains in tolerable amplitudes with a steady characteristics. In both cases, the amplitude of error signal is given in Table 5.2. Since those systems

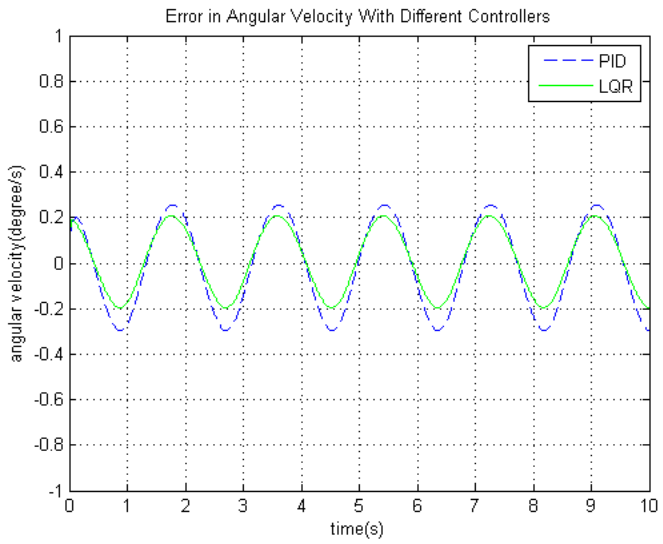

Figure 5.11: Error in Tracking of Sinusoidal Signal with an Amplitude of 30 deg/s which Corresponds to the Maximum Angular Velocity Change of Rhex Signal with Robot Speed Set to 0.3.

Table 5.3: Experimental Oscillations Values of Robot Base at Different Robot Speed.

Robot Speed	Oscillation Period	Oscillation Amplitude(peak to peak)
0.3	1.827s	60 degree/s
0.6	1.108s	90 degree/s
0.9	0.656s	120 degree/s

are able to track the signal with that amplitude, both controller failed while trying to track a virtual $\dot{\phi}$ which has similar amplitude and frequency as the experiment at velocity is set to 0.9.

However both controllers can not manage to track the sinusoidal signal which corresponds to the experiment with the highest robot speed. So at this velocity level of the robot, success rate of the controller could be assumed to be low.

Robot Speed	Error in PID	Error in LQR
0.3	0.25 degree/s	0.2 degree/s
0.6	0.6 degree/s	0.5 degree/s
0.9	FAIL	FAIL

Table 5.4: Errors Amplitude in Tracking the Sinusoidal Signal at Different Robot Speed.

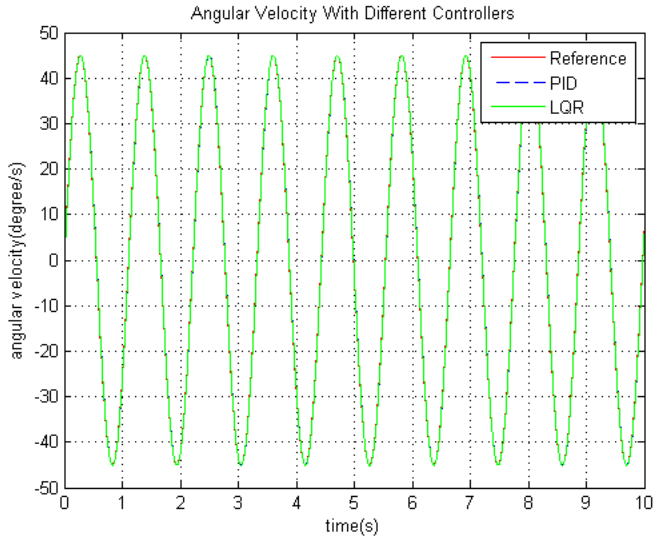

Figure 5.12: Tracking of Sinusoidal Signal with an Amplitude of 45 deg/s which Corresponds to the Maximum Angular Velocity Change of Rhex Signal with Robot Speed Set to 0.6.

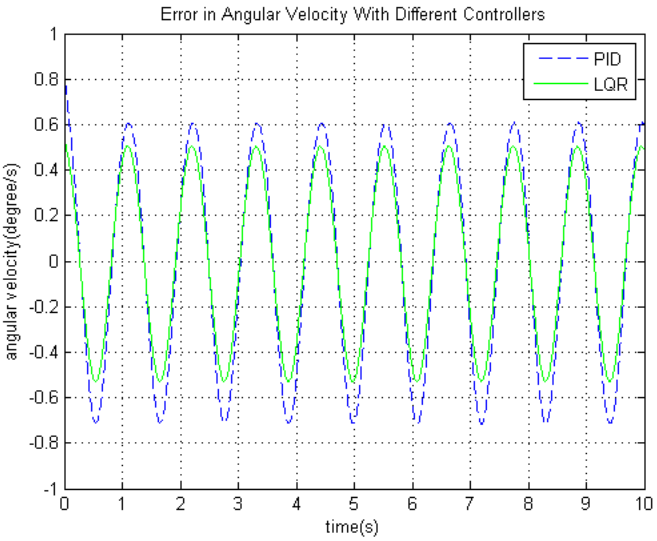

Figure 5.13: Error in Tracking of Sinusoidal Signal with an Amplitude of 45 deg/s which Corresponds to the Maximum Angular Velocity Change of Rhex Signal with Robot Speed Set to 0.6.

5.3 Tracking the Angular Movement of Rhex

Main motivation behind this study is to design a head stabilization platform for our robot SensoRHex, so that the effect of angular disturbances due to the legged locomotion of the robot must be minimized. This results performance increase in image processing algorithms since the main load of the head stabilization platform will be a camera.

Figure 5.14: Microstrain Inertial Measurement Unit used to Obtain Angular Velocity and Acceleration in Rhex Robot.

In order to design a platform as mentioned first of all the angular disturbances must be investigated during robot motion. Several experiments are conducted and angular motion data is taken by using MicroStrain 3DM-GX1 inertial measurement unit(Fig. 5.14). Three experimental data arrays are obtained from those trials with different forward velocities. Those experiments are conducted at robot speed set to 0.3, 0.6 and 0.9.

Fig. 5.15 is the velocity data taken from the IMU sensor during the motion of the robot when the speed of the robot is set to 0.3. As expected the maximum change occurs in pitch axis. Since our head/camera stabilization platform is a planar version which is capable of canceling the disturbances occurs in only one axis, the changes in the pitch axis is selected and performance of controllers are tested by using the pitch axis signal.

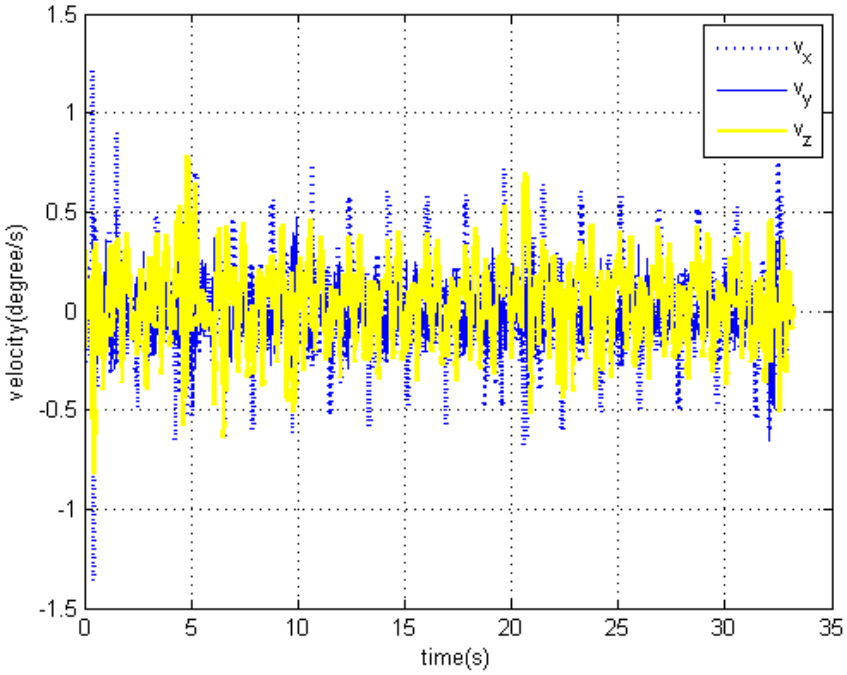

Figure 5.15: Velocity Graph of All Axis.

Starting point of this study was the need of increasing the image data quality taken from the camera which is mounted on the robots body. Due to non-ideal practical issues, like motion blur, performance of image processing algorithms are decreased. A hardware solution is proposed as a head stabilization platform for this problem. Also, because the origin of this problem is caused by the changes in angular velocity, aim of this study is focused on stabilizing the angular velocity of the head platform. Experiments are conducted with our robot Rhex and angular velocity and angular acceleration data are obtained by using an IMU sensor at three different robot speeds. Fig. 5.17 shows the picture of sensors mounted on the robot. Fig. 5.16 illustrates the angular velocity in pitch axis measured on Rhex during locomotion with the speed set to 3. Since there will be a passive isolation system at the bottom of the stabilization platform, red lines in Fig. 5.16 shows the angular velocity of the stabilization platform after passive isolation is applied where blue graph shows the row velocity data.

Angular velocities at the robot body due to locomotion at different speeds is given in Fig. 5.18 after passive isolation. The effect of passive isolation could be clearly seen with comparing Fig. 5.18 and Fig. 5.4, where filtered and non-filtered angular velocity

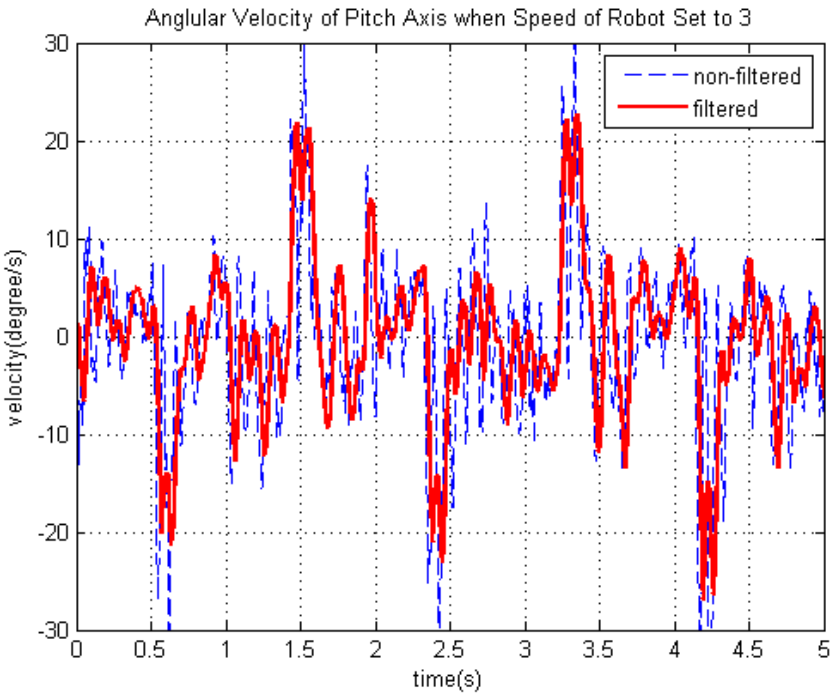

Figure 5.16: Angular Velocity of Pitch Axis with Robot Speed set to 3 with and without Passive Isolation.

values are illustrated. This section presents results of controlling directly the angular velocity of the robot with PID and LQR controllers with three different motor, M1270, M2070 and an ideal Motor. Comparative results for all three experiments are given in Fig. 5.19 , Fig. 5.21 and Fig. 5.21 for M1270. Since M2070 is a more powerful motor, better results are obtained in Fig. 5.25 , Fig. 5.27 and Fig. 5.27.

Moreover angular velocity errors of controller while tracking the experimental signals are given in Fig. 5.20, Fig. 5.22 and Fig. 5.24 and Fig. 5.26, Fig. 5.28 and Fig. 5.30 for both motors. Since those motors have certain peak force values as the control effort increases above their maximum force values saturation occurs. However ideal motor is free from this case and angular velocity error during experiments with different speed of our robot is given in Fig. 5.31, Fig. 5.32 and Fig. 5.33. In addition Table 5.3 shows the value of maximum error in angular velocity in all cases.

Simulations with an ideal motor shows us that, although controller are able, disturbance rejection capability of the system is limited by the motor type. Also in the case where the robot speed is set to 0.9, the disturbance cancellation results are unsuccess-

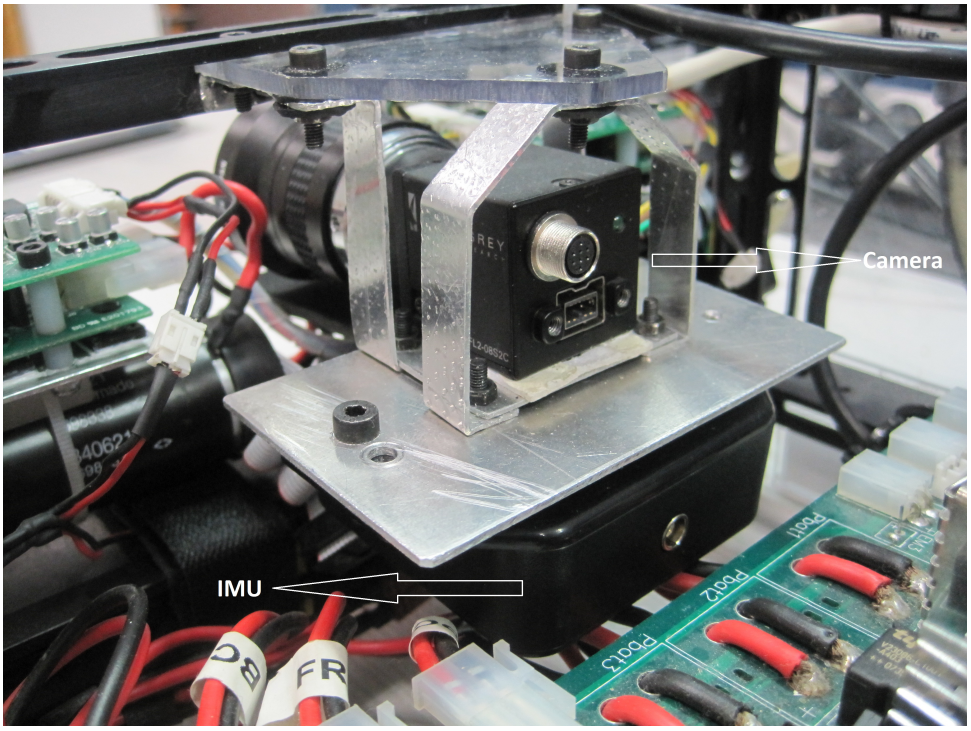

Figure 5.17: Locations of Inertial Measurement Unit and Camera on RHex.

Table 5.5: Maximum and Average Amplitude Errors (degree/s) in Tracking the Experimental Signals Taken From Rhex with IMU during locomotion at Different Robot Speeds.

Motor Type	Vel. Set to 0.3	Vel. Set to 0.6	Vel. Set to 0.9
M1270	max = 20 / av = 1.61	max = 25 / av = 3.27	max = 40 / av = 12.97
M2070	max = 4 / av = 0.37	max = 10 / av = 0.63	max = 30 / av = 5.30
Mideal	max = 2/ av = 0.37	max = 4 / av = 0.49	max = 5 / av = 1.04

ful as predicted in Section 5.2. Also from Table 5.3 it is clear that both motors can cancel out disturbances occurs when robot speed is set to 0.3 and 0.6 however at the highest robot speed, peak force values of the motors are exceeded in order to manage effective stabilization. The main reason behind the result with the ideal motor case is that the assumption of infinity peak force value.

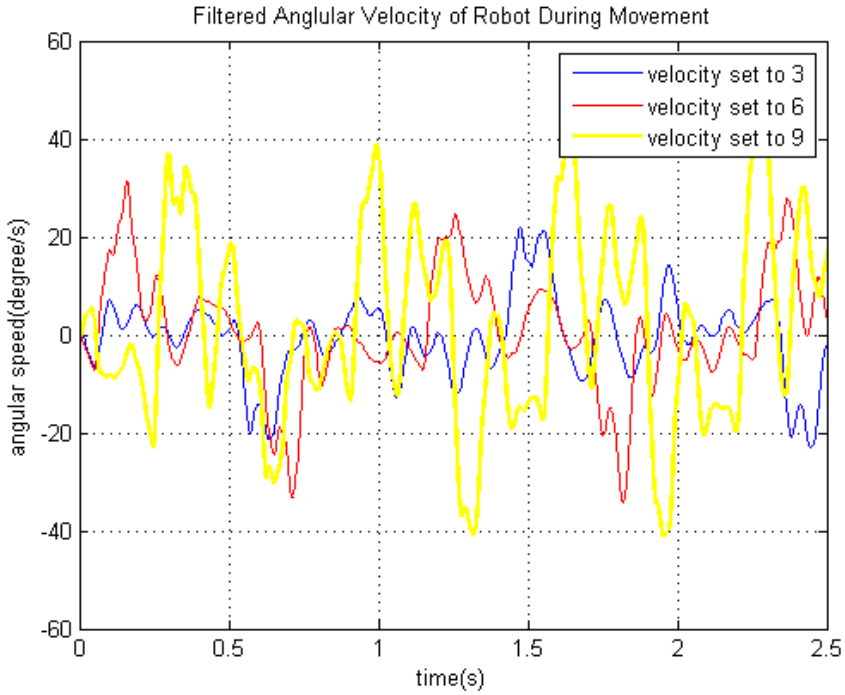

Figure 5.18: Angular Velocities of the Robot Body in Three Different Robot Speed.

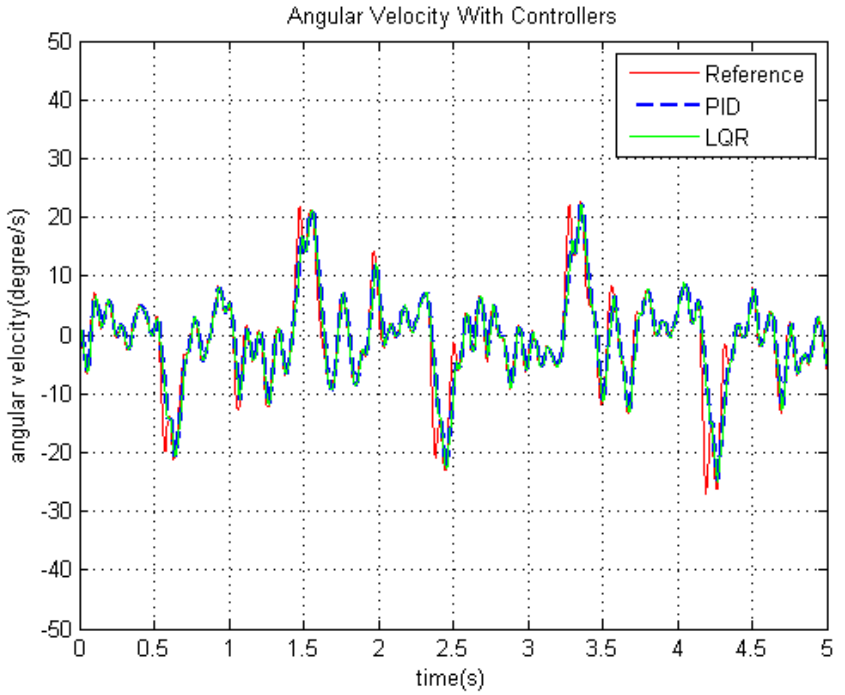

Figure 5.19: Tracking of Experimental Angular Velocity with the Robot Speed Set to 0.3 with Linear DC motor M1270.

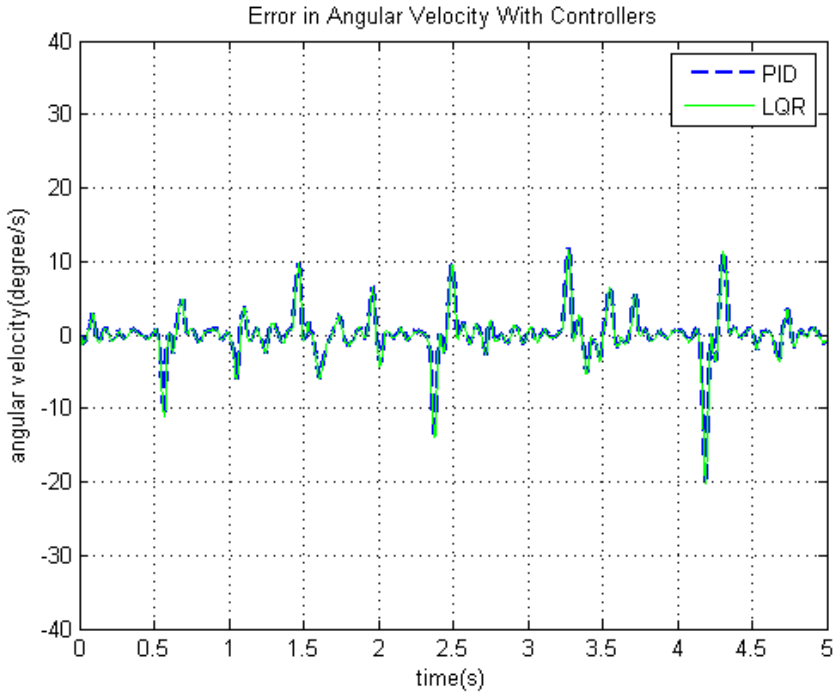

Figure 5.20: Error in Tracking of Experimental Angular Position with the Robot Speed Set to 0.3 with Linear DC motor M1270.

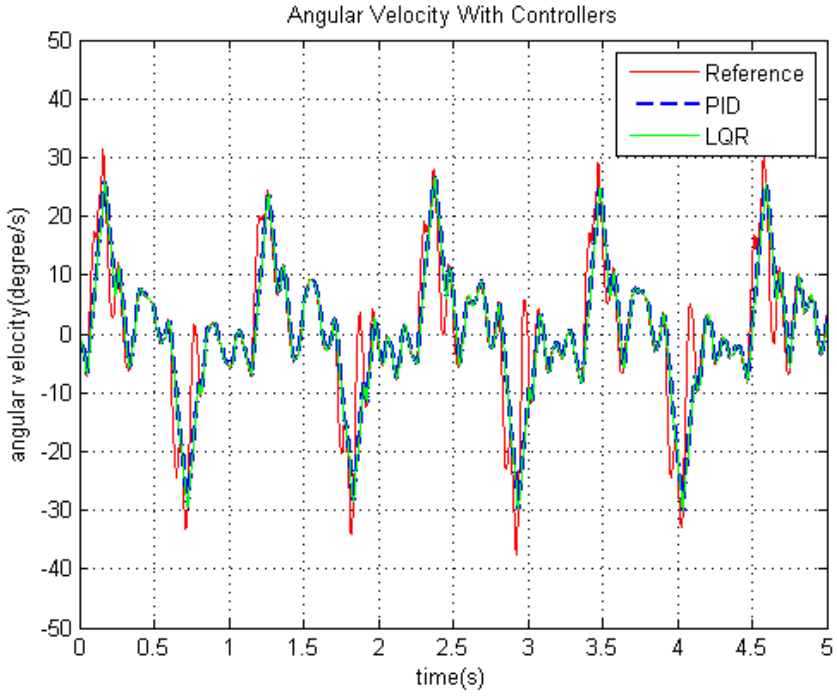

Figure 5.21: Tracking of Experimental Angular Velocity with the Robot Speed Set to 0.6 with Linear DC motor M1270.

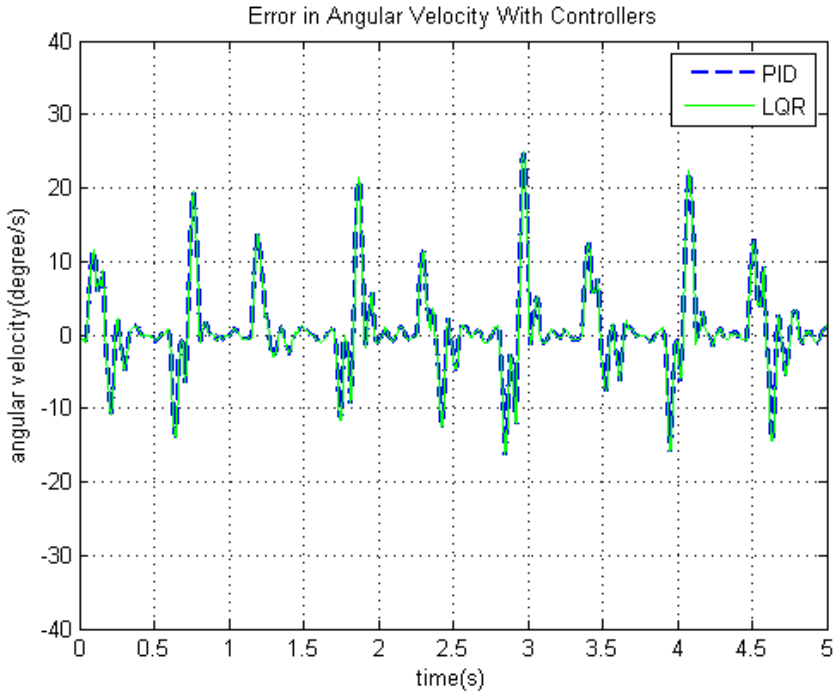

Figure 5.22: Error in Tracking of Experimental Angular Position with the Robot Speed Set to 0.6 with Linear DC motor M1270.

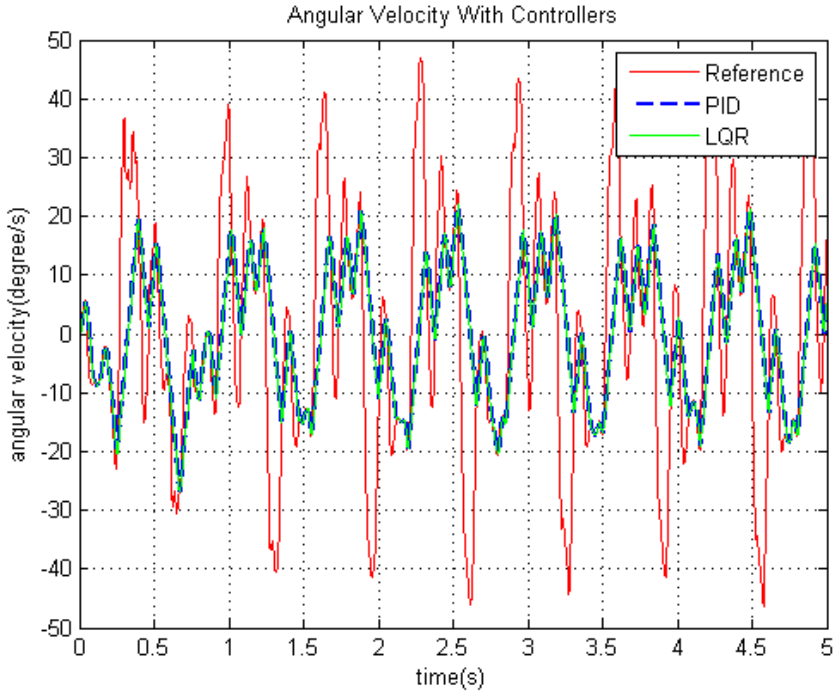

Figure 5.23: Tracking of Experimental Angular Velocity with the Robot Speed Set to 0.9 with Linear DC motor M1270.

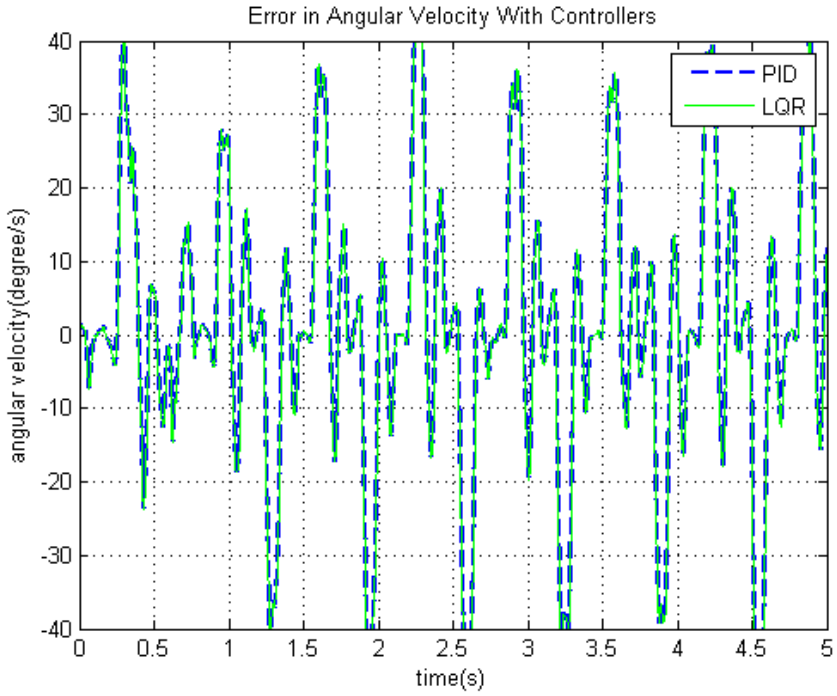

Figure 5.24: Error in Tracking of Experimental Angular Position with the Robot Speed Set to 0.9 with Linear DC motor M1270 .

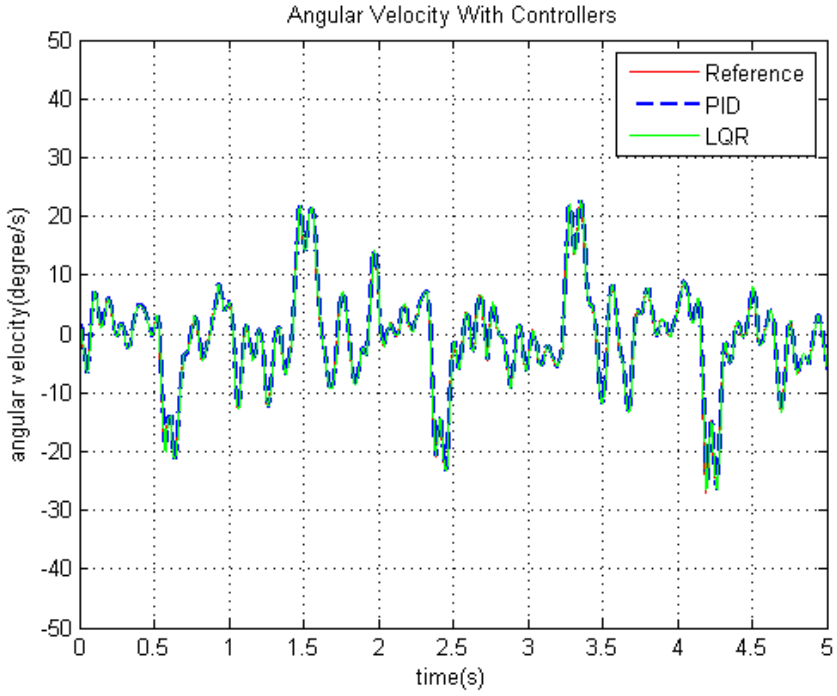

Figure 5.25: Tracking of Experimental Angular Velocity with the Robot Speed Set to 0.3 with Linear DC motor M2070.

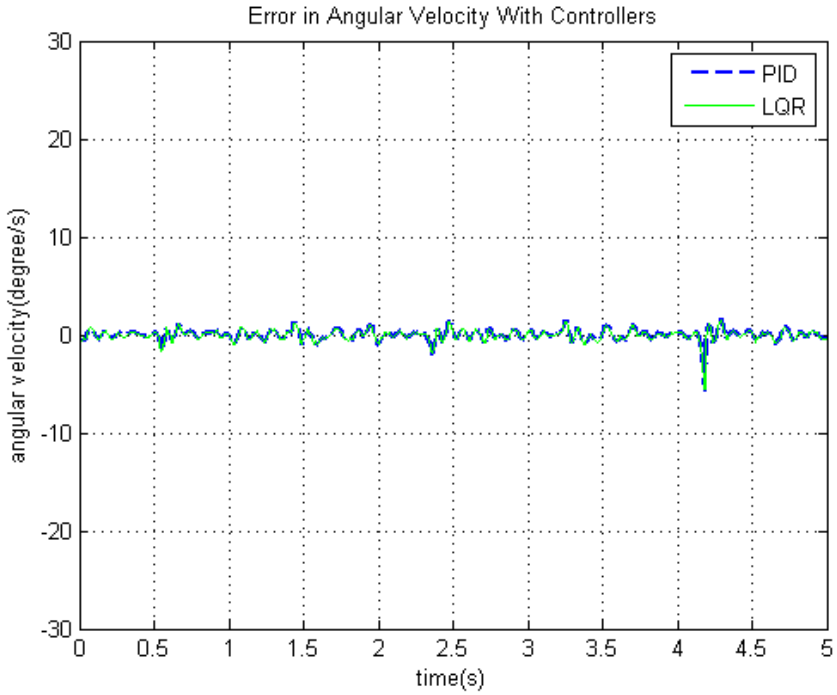

Figure 5.26: Error in Tracking of Experimental Angular Position with the Robot Speed Set to 0.3 with Linear DC motor M2070.

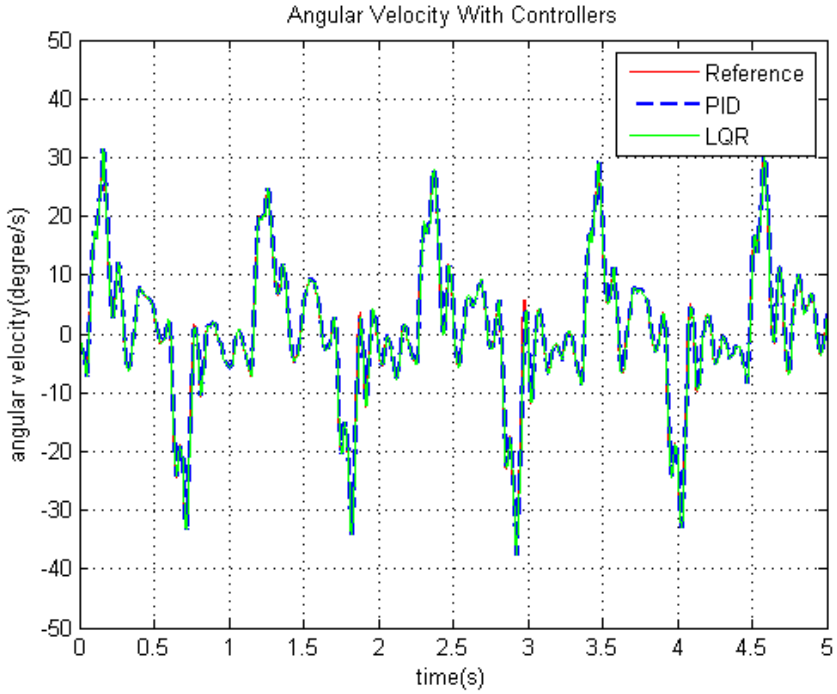

Figure 5.27: Tracking of Experimental Angular Velocity with the Robot Speed Set to 0.6 with Linear DC motor M2070.

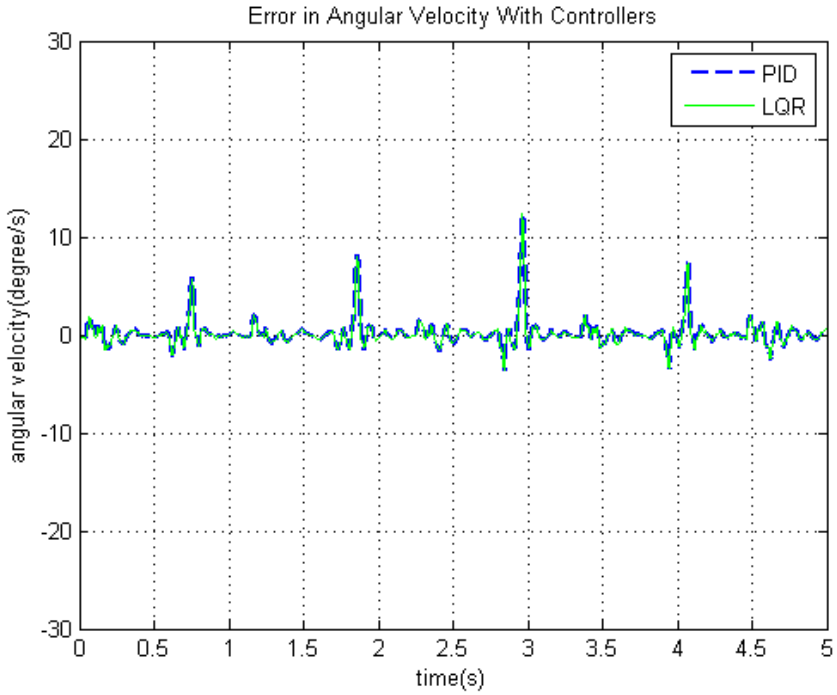

Figure 5.28: Error in Tracking of Experimental Angular Position with the Robot Speed Set to 0.6 with Linear DC motor M2070.

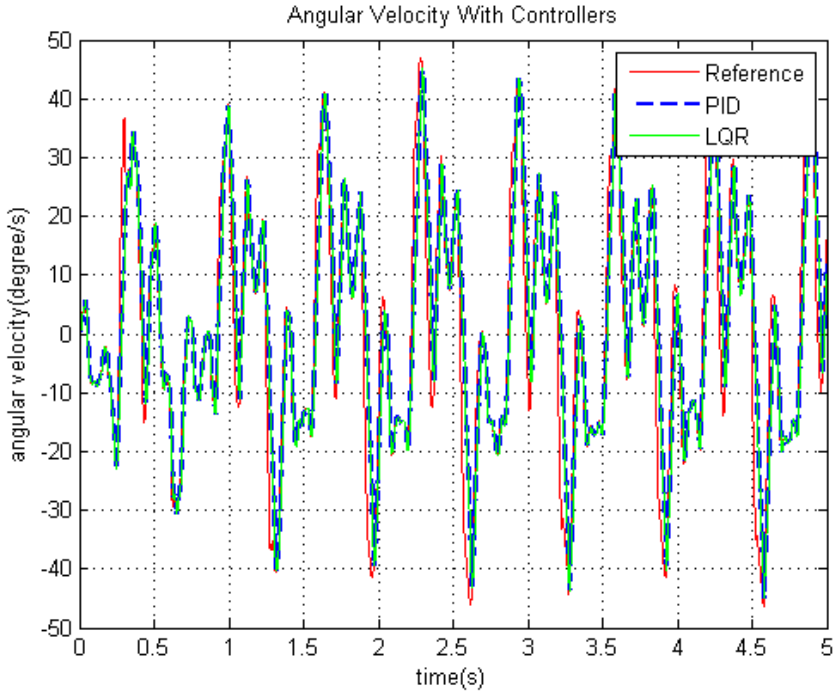

Figure 5.29: Tracking of Experimental Angular Velocity with the Robot Speed Set to 0.9 with Linear DC motor M2070.

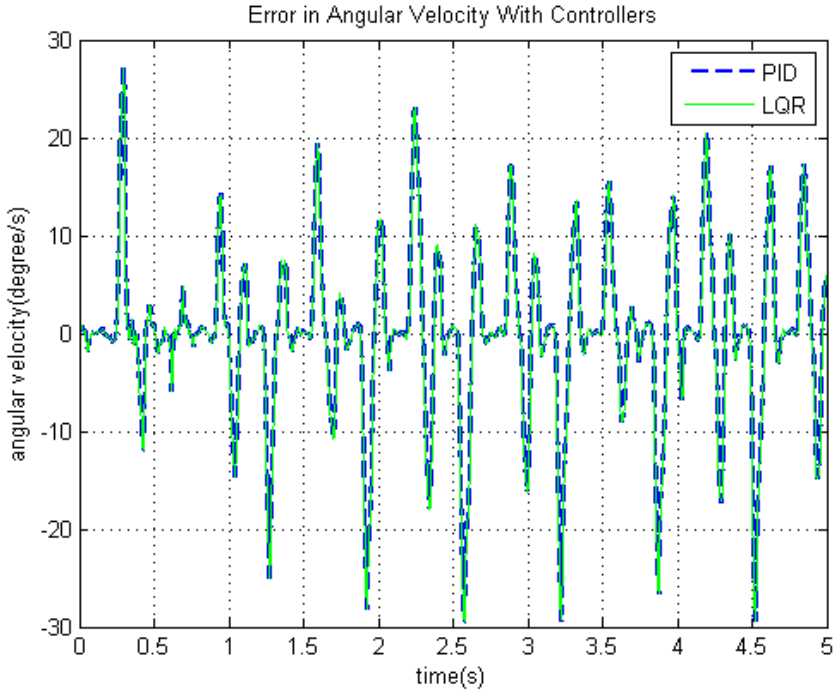

Figure 5.30: Error in Tracking of Experimental Angular Position with the Robot Speed Set to 0.9 with Linear DC motor M2070.

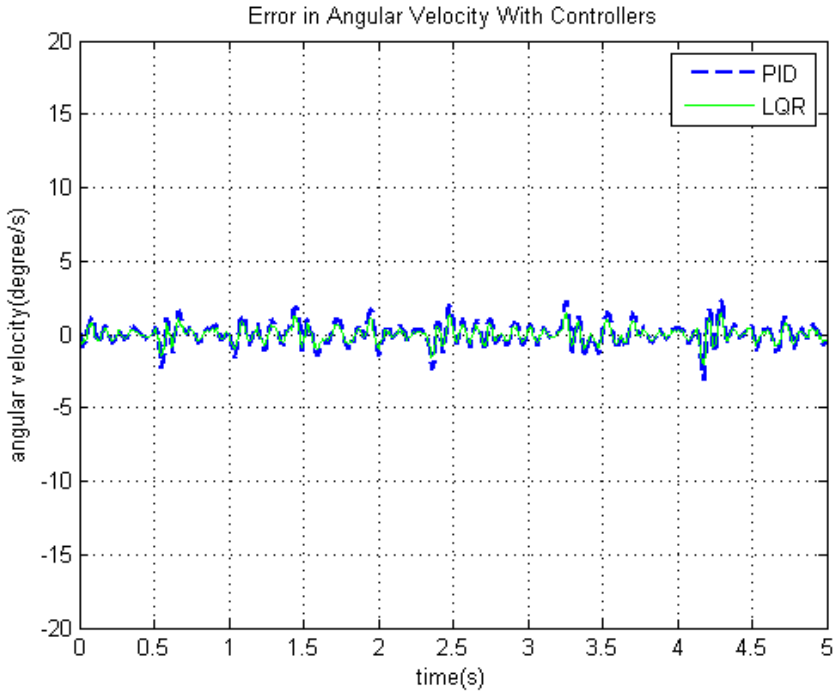

Figure 5.31: Error in Tracking of Experimental Angular Position with the Robot Speed Set to 0.3 with an ideal motor.

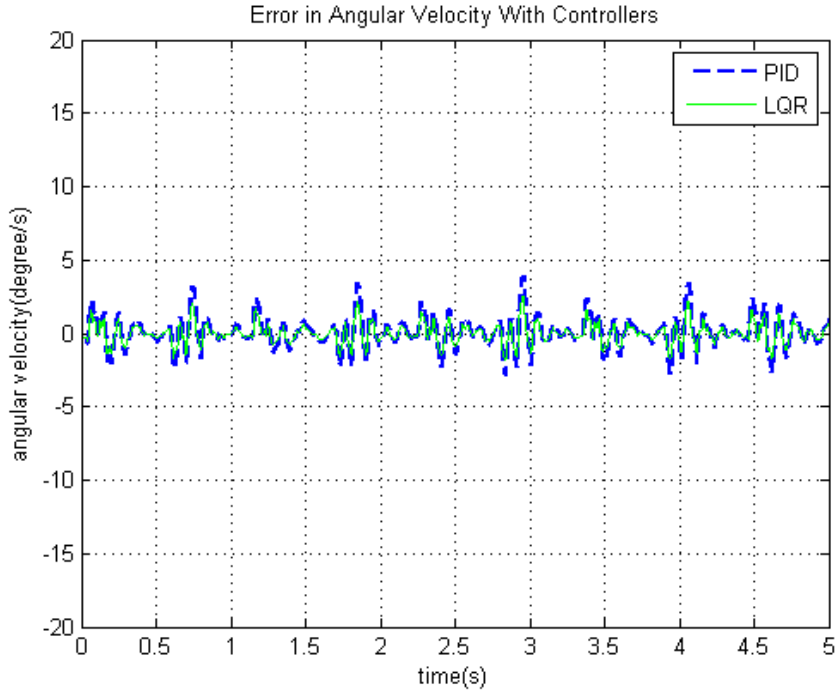

Figure 5.32: Error in Tracking of Experimental Angular Position with the Robot Speed Set to 0.6 with an ideal motor.

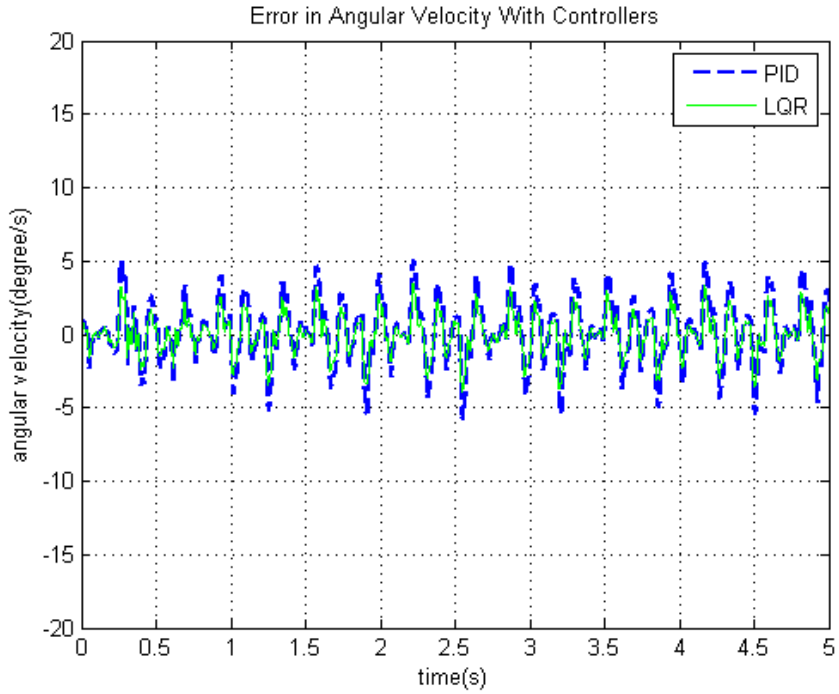

Figure 5.33: Error in Tracking of Experimental Angular Position with the Robot Speed Set to 0.9 with an ideal motor.

5.4 Performance Evaluation with Different Motors

From the above discussions, the case when the control parameter is selected as the angular velocity. However it is noted that a weight comparatively small with the velocity must be given to the angle of the pendulum. Also the most important parameter that effects the controller performance is the motor selection. In the head stabilization platform a Faulhaber linear DC motor will be used Fig. 5.34. However there exists three different motors with all different parameters. As the motors maximum peak force increases the disturbance cancellation performance of the model increases significantly. But as a trade of motors size,weight and power consumption increases proportionally. Table 5.6 summarizes some important parameters of the motors.

Figure 5.34: Faulhaber Linear DC Motor Used in Head Stabilization Platform

With a set of different control parameters simulations with those motors models are conducted in order to determine the most suitable one. So results with LM0830, LM1247 and LM2070 are given comparatively and their feasibility in head stabilization platform is discussed.

In an ideal motor peak force is assumed to be infinity, which means that as the voltage applied to the motor increases, the produced force will also have the same tendency. However in real life application, motors can not exceed their peak force value. Also if a motor produces its peak force for a certain amount of time due to the temperature rise in the motor core, permanent damage could occur in the motor. So this incident must also be taken in to consideration during the motor selection.

Table 5.6: Parameters of Different Faulhaber Linear DC Motors.

Motor Type	Cont. Force	Peak Force	Peak Current	Force Constant	Length	Weight
LM0830	1.03 N	2.74 N	1.41 A	1.94 N/A	27 mm	17 g
LM1247	3.6 N	10.7 N	1.66 A	6.43 N/A	46.8 mm	82 g
LM2070	9.2 N	27.6 N	2.37 A	11.64 N/A	70 mm	388 g

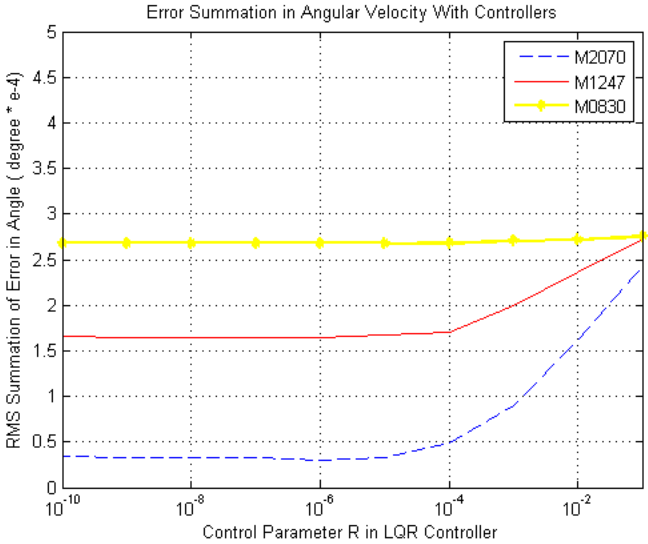

Figure 5.35: Summation of Mean Squared Error with Different Control Parameters R for All Kinds of Faulhaber Motors During Robot Locomotion Velocity Set to 0.3

It obvious that as the amount of the force applied to the system increases the controllers performance will increase however since every motor can produce a certain amount of maximum torque. Force saturation will occur when the controller asks for a force output greater than the peak value of that motor. This saturations results nonlinearities in control, which will limit the control performance. At Fig. 5.35, Fig. 5.36 and Fig. 5.37 this effect is observed clearly for all experimental angular velocity values measured from our robot RHex. Those figures shows the summation of rms error for a certain R value in LQR control for three different motors which have

Table 5.7: Summation of RMS Error in Angular Velocity in terms of degrees*10^{-4} During Robot Locomotion Velocity Set to 0.3

Motor Type	R = 10^{-1}	R = 10^{-3}	R = 10^{-4}	R = 10^{-5}	R = 10^{-6}	R = 10^{-8}	PID
LM0830	5.58	5.13	5.10	5.07	5.11	5.12	5.10
LM1247	4.39	1.20	0.842	0.781	0.811	0.830	0.822
LM2070	2.67	0.117	0.052	0.139	0.148	0.160	0.130

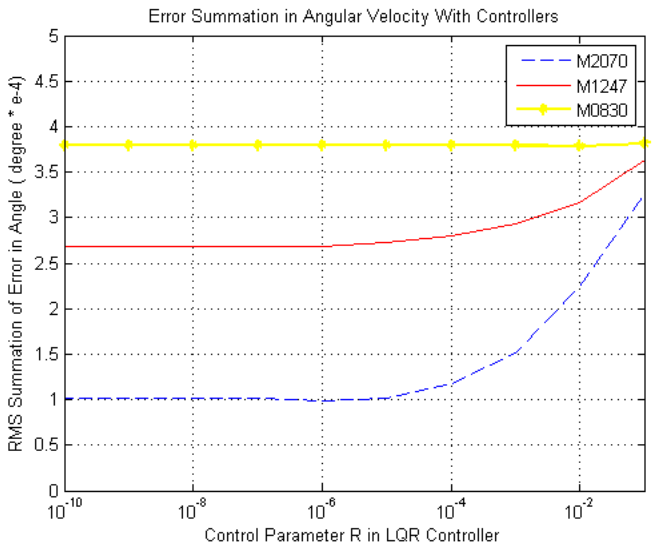

Figure 5.36: Summation of Mean Squared Error with Different Control Parameters R for All Kinds of Faulhaber Motors During Robot Locomotion Velocity Set to 0.6

Table 5.8: Summation of Mean Squared Error in Angular Velocity in terms of degrees*10^{-4} During Robot Locomotion Velocity Set to 0.6

Motor Type	R = 10^{-1}	R = 10^{-3}	R = 10^{-5}	R = 10^{-6}	R = 10^{-8}	PID
LM0830	3.82	3.80	3.80	3.80	3.80	3.80
LM1247	3.64	2.93	2.73	2.69	2.69	2.70
LM2070	3.27	1.51	1.01	0.98	1.01	1.04

different maximum peak values. As R decreases the control effort increases directly in LQR controller. However in PID control there exist no such direct relation with the control parameter and the control effort. So LQR control is most suitable for this comparison. It is expected that as R decreases the summation of rms error will decrease also. However since force saturation occurs after a certain point, despite an decrease in R do not results any performance increase.

In Table 5.7, Table 5.8 and Table 5.9 the values of summation error for different

Table 5.9: Summation of Mean Squared Error in Angular Velocity in terms of degrees*10^{-4} During Robot Locomotion Velocity Set to 0.9

Motor Type	R = 10^{-1}	R = 10^{-3}	R = 10^{-5}	R = 10^{-6}	R = 10^{-8}	PID
LM0830	8.71	8.75	8.75	8.75	8.74	8.72
LM1247	8.04	8.08	8.09	8.09	8.09	8.09
LM2070	7.02	6.00	5.75	5.71	5.74	5.67

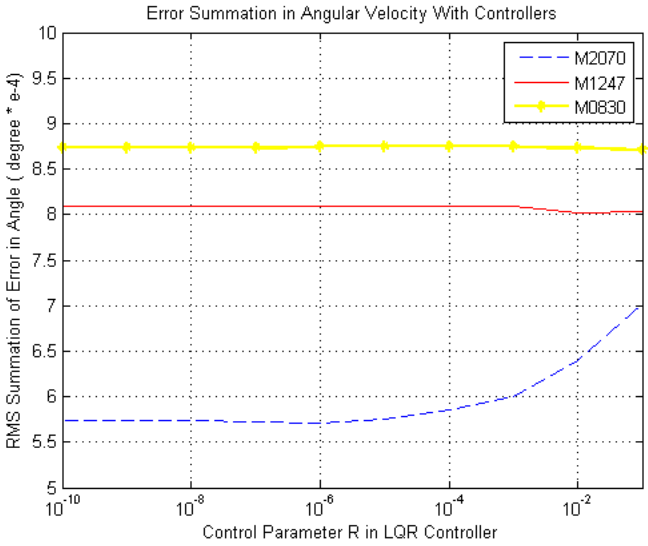

Figure 5.37: Summation of Mean Squared Error with Different Control Parameters R for All Kinds of Faulhaber Motors During Robot Locomotion Velocity Set to 0.9

control parameters for different motor types are given. From those values one can also observe that after a certain R value, there is no change in the summation of error. The effect of saturation in the motor force is observed by investigating the gray shaded sections in Table 5.7. Fig. 5.38 and Fig. 5.40 shows the angular velocity error while Fig. 5.39 and Fig. 5.41 are the force output at those experiments. Force saturation, which limits the controller performance is clear when R is small.

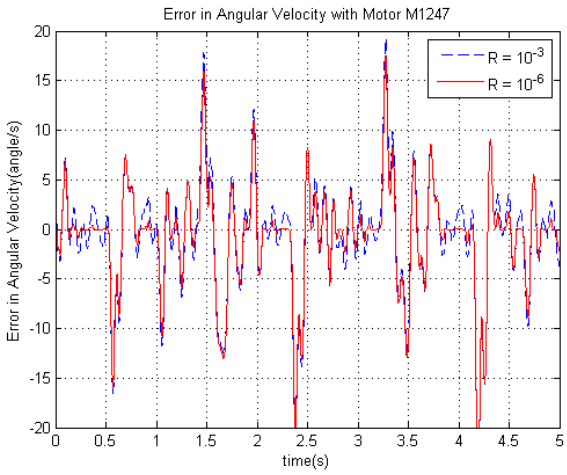

Figure 5.38: Angular Velocity Error with Different Control Parameters R for M1247 Faulhaber Linear Motor During Robot Locomotion Velocity Set to 3

However results with bigger motor M2070 is much more superior than M1247, dimen-

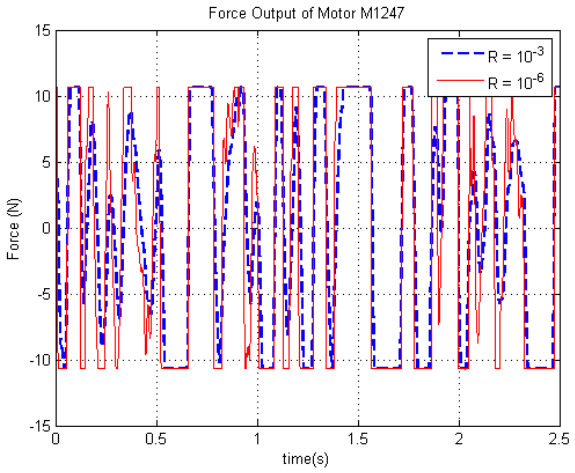

Figure 5.39: Force Output of M1247 Faulhaber Linear Motor During Robot Locomotion Velocity Set to 0.3 with Different Control Parameters R

sion and weight of bigger motor is a problem. If both motors are evaluated in terms of weight there is 300g difference between them. Since the platform will be mounted on robot RHex this amount of weight could decrease the locomotion performance of our robot when it is considered that the actual three axes head stabilization platform will consists of three motors. So from above discussions M1247 is considered as a more suitable for our system.

Also using a motor in its peak force value for a certain amount of time could damage the motor permanently, so while choosing the control parameters, the duration of applied peak force must be taken into consideration. And due to the trade of between the performance of the system and risk of permanent damage in the motor, a lesser control input which results more angular velocity error could be selected for the sake of the motor.

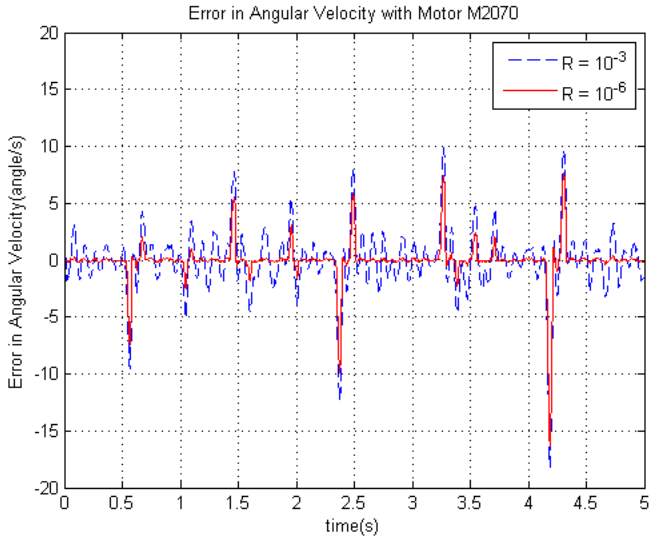

Figure 5.40: Angular Velocity Error with Different Control Parameters R for M2070 Faulhaber Linear Motor During Robot Locomotion Velocity Set to 3

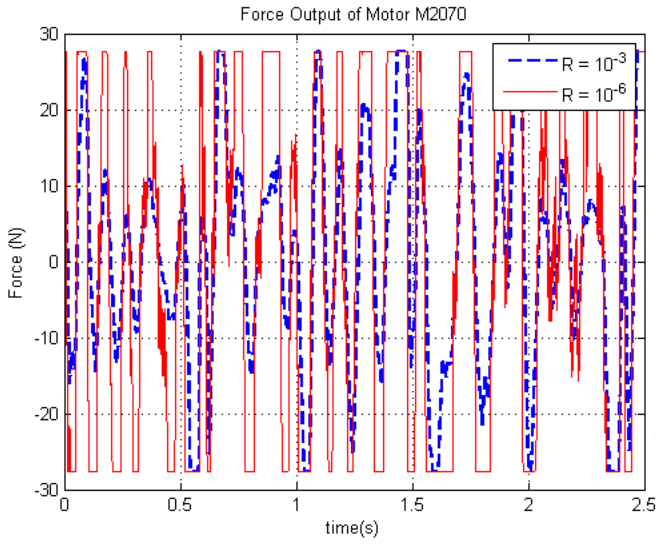

Figure 5.41: Force Output of M2070 Faulhaber Linear Motor During Robot Locomotion Velocity Set to 0.3 with Different Control Parameters R

5.5 Relation Between Motion Blur and Robot Motion

As mentioned though the thesis, main motivation behind this study is to implement a camera stabilization platform for our robot Rhex, which cancels outs the angular disturbances due to the legged locomotion. This stabilization platform will increase the image processing algorithms that are running on the SensoRHex by reducing the motion blur. As illustrated in Fig. 5.42 the relation between controller and the angular velocity (1), is derived in this section. Moreover the relation between the motion blur and the feature detection failure in edge,corner and sift algorithms (2) are derived in the thesis of another member of our ROLAB(Robotics Labrotory Group in METU EE) [43]. By roughly estimating the relation between the angular velocity and motion blur (3), we can have more insight about the effect of controlling the angular velocity in image processing algorithms.

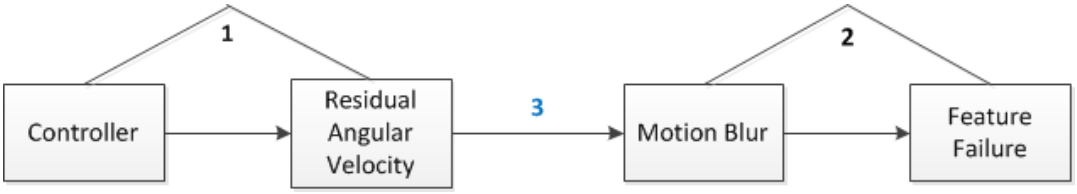

Figure 5.42: Relation Diagram of Controller Angular Velocity Motion Blur and Feature Detection.

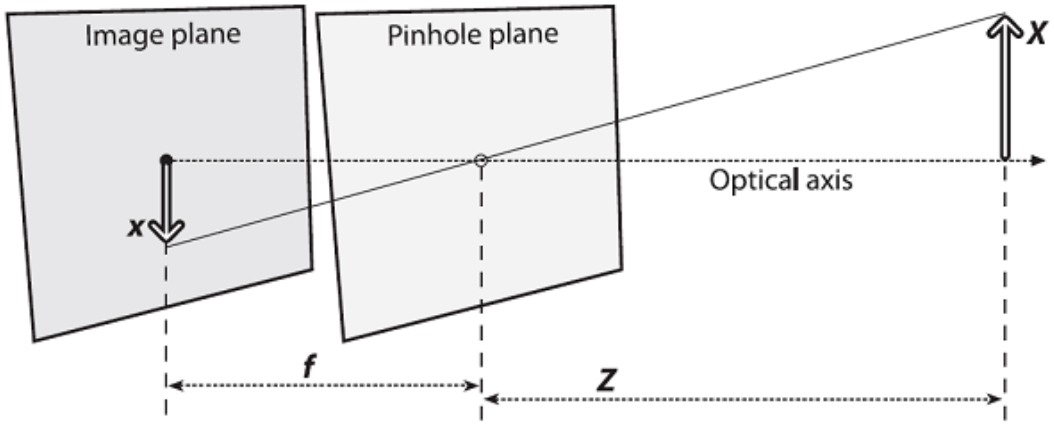

Figure 5.43: Pin Hole Camera Model.

By taking the pinhole camera model into consideration as Fig. 5.43, the relation between the angular velocity and motion blur in terms of pixels are derived. Moreover

Table 5.10: Maximum and Minimum Amount of Motion Blur in term of Pixels for an angular velocity of 1 degree/s with a shutter speed of 1/60 s

Angular Velocity	Minimum Motion Blur	Maximum Motion Blur
1 degree/s	0.38 pixels	0.40 pixels

Table 5.11: Maximum and Minimum Amount of Motion Blur in term of Pixels for an angular velocity of 1 degree/s with a shutter speed of 1/60 s with Linear Motor M1247

Robot Speed	Max. Error	Motion Blur	Abs. Average Error	Average Motion Blur
Set to 0.3	20 degree/s	7.6 pixels	2.09 degree/s	0.836 pixels
Set to 0.6	25 degree/s	9.5 pixels	3.65 degree/s	1.46 pixels
Set to 0.9	40 degree/s	15.2 pixels	13.1 degree/s	5.24 pixels

camera intrinsic parameters are used for this calculation which are derived experimentally by using camera calibration algorithms. Experimental focal length of the Flea 2 camera is found ad 9.731 mm, where a pixel has the dimensions of $7.4x7.4$ micrometers. And by estimating the shutter speed of the camera to 1/60 s and the distance between the object and the robot will be 5m, the minimum and maximum amount of occurred motion blur is approximated as 0.38 and 0.40 pixels as seen from Table 5.10.

By combining the knowledge with the thesis study, motion blur during the locomotion of Rhex at different speeds could be estimated. Table 5.11 and Table 5.12 shows the predicted motion blur in terms of pixels during locomotion while Flea2 is used as the camera. Also from this results one can conclude that in order to obtain qualified image data, images must be taken at most when robot speed is set to 0.6.

Table 5.12: Maximum and Minimum Amount of Motion Blur in term of Pixels for an angular velocity of 1 degree/s with a shutter speed of 1/60 s with Linear Motor M2070

Robot Speed	Max. Error	Motion Blur	Abs. Average Error	Average Motion Blur
Set to 0.3	4 degree/s	1.6 pixels	0.37 degree/s	0.148 pixels
Set to 0.6	10 degree/s	4 pixels	0.63 degree/s	0.252 pixels
Set to 0.9	30 degree/s	12 pixels	5.30 degree/s	2.12 pixels

5.6 Additional Conditions Effects the Performance

Note that main motivation behind this study is the improve the image quality taken from our robot Rhex. In order to achieve this task the design of a single axis disturbance cancellation platform is investigated in this study which is a preliminary work for a three axis head or camera stabilization platform. During this study results shows that as the **locomotion speed** of the robot increases angular velocity disturbances increases significantly which results the demand of a higher control effort.

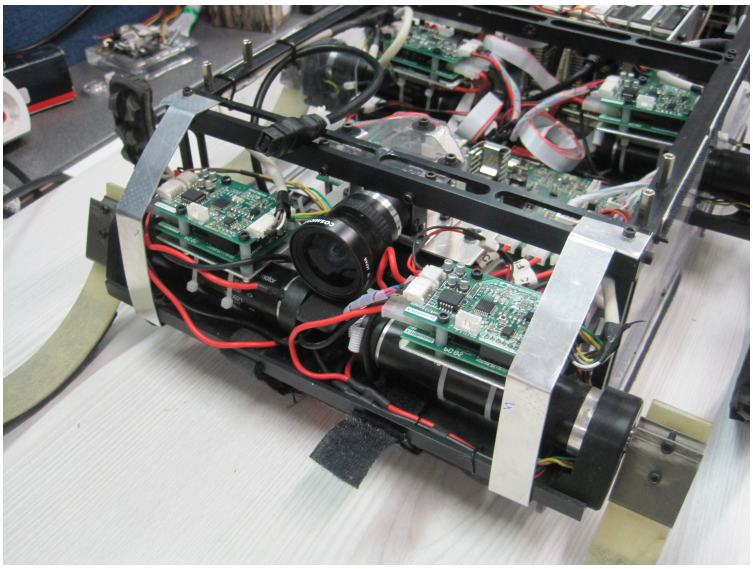

Figure 5.44: Flea 2 Camera Mounted on SensoRHex

However shutter speed parameter of the camera is directly proportional to the motion blur concept. If the shutter speed is in millisecond scale the motion blur an the image will be negligible but it the shutter speed is set to once second, camera must stay stabilize during that one second in order to obtain a qualified image data. As Fig. 5.44 illustrated the camera on the SensoRHex is a Flea 2 which has a shutter speed variable between 0.02ms to 10s.

In addition, the **illumination of light** in the environment effects directly the performance of the camera in terms of the need of shutter speed, in a brighter area shutter speed could be lower with compared to a darker area, in order to obtain the same image quality. So in darker places control effort must be higher due to high shutter speed. The above mentioned phenomenons are illustrated in Fig. 5.45 graphically.

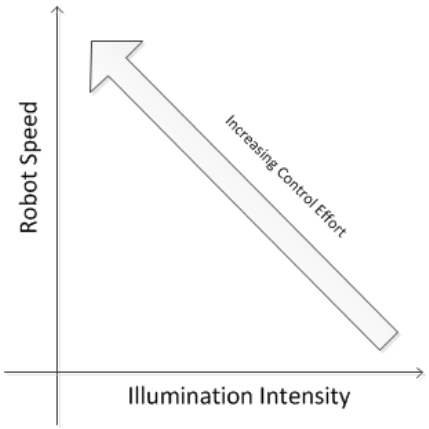

Figure 5.45: Graphic Illustration of the Relation Between Robot Speed and Illumination Intensity to Control Effort

Table 5.13: Effect of sampling period to the controller performance

Sampling Period	Absolute Average Error
20 ms	4.59 degree
2 ms	1.34 degree
0.2 ms	1.14 degree
0.02 ms	0.16 degree

Moreover the **sampling period** of the controller is a crucial parameter which effects the performance. During this study the sampling period of the controller is selected as 200Hz which could be achieved by an advanced micro controller. However as the sampling period decreases a significant increase in the stabilizing performance is observed. Table 5.6 illustrates the effect of sampling period when controller is stabilizing the angular movements of SensoRHex at robot speed is set to 3 with the motor M1247.

Actuator mounting angle (α) directly effects the applied force to the camera platform since there is a trigonometric relation between. As seen in Fig. 5.46, it is more clear that as the mounting angle decreases, the effect of applied force is reduced exponentially. So during hardware design, in the light of this parameter the mounting angle is tried to be selected as small as possible within mechanical constraints. Also Table 5.6 illustrates this phenomenon numerically.

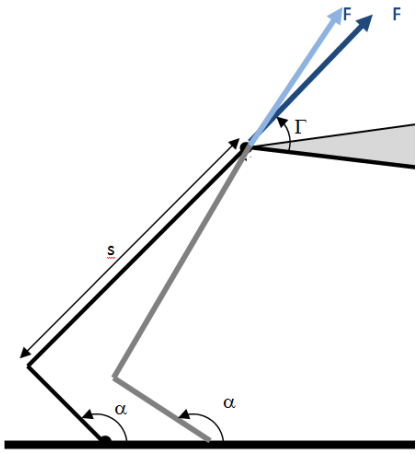

Figure 5.46: Graphic Illustration of the actuator mounting

Table 5.14: Effect of mounting angle of the actuator to the controller performance

Mounting Angle	Absolute Average Error
170 degree	1.23 degree
125 degree	2.59 degree
110 degree	3.87 degree

5.7 Discussion

This chapter gives the detailed analysis of the head or camera stabilization model with several conditions. Both PID and LQR controller are implemented in order to track the disturbance signals where sinusoidal and real life experimental angular velocity data measures on the SensoRHex during locomotion is used. In it concluded that if the controller can track a signal successfully than it can reject those signals when they are applied as disturbance to the system. Moreover both controllers give successful results.

Then the effect of motor selection and parameter selection is mentioned at this stage. Results clearly shows that as the peak force output of the motor increases the control performance of the system increases. And also since as the robot speed increases the oscillations on the body increases, control becomes more difficult.

So usage of linear DC motor M2070 will absolutely increase the disturbance rejection performance of the system an will result much less motion blur in the image. However the size, weight and power consumption of that motor is relatively high. On the other hand M1247 gives acceptable results while speed of the robot is set to 3 and 6. So during the usage of the image processing data speed of the robot could be decreased.

Moreover if the angular error figures are analyzed, it is obvious that angular velocity peak occurs at the instance when the leg of the robot touches to the ground, other than this movement angular velocity error is relatively very low. As seen in Fig. 5.47 which is the performance of the M1247 motor during the locomotion of the robot when the speed is set to 3, dotted points represents the high peak error when the leg of the robot touches to the ground. Since our shutter speed will be around 1/60 many image datas could be taken between those dotted areas. So by measuring the residual angular velocity of the upper platform the the head model, and implementing a controllable image obtaining system or by simply neglecting the image data taken at the instance above a certain residual angular velocity a much better image processing performance could be obtained.

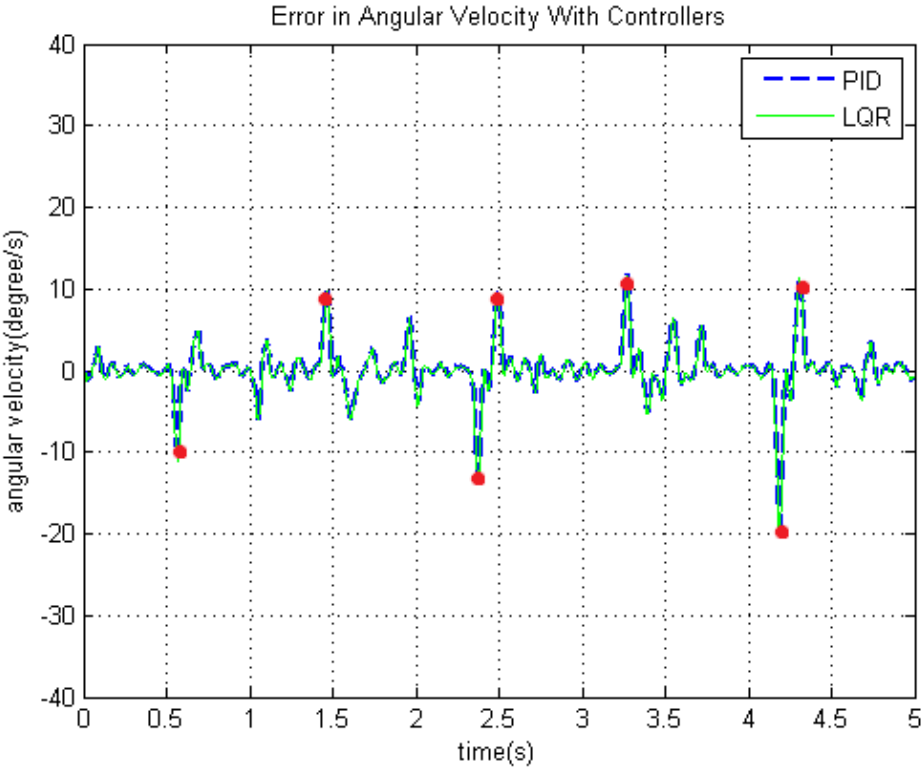

Figure 5.47: Error in Tracking of Experimental Angular Position with the Robot Speed Set to 0.3 with Linear DC motor M1247 with Peak Errors are Marked.

CHAPTER 6

CONCLUSION AND FUTURE WORK

Main motivation behind this study is to design a head stabilization platform which can cancel the oscillations in the body occurred due to the legged motion of our robot SensoRHex. Angular velocity changes on the robot body cause non-ideal results in sensors especially in the camera. Motion blur during the locomotion, effects the feature detection performance of image processing algorithms occurs as a results of this motion. Although those oscillations presents in all axis, roll, yaw and pitch. A planar head stabilization system which is capable of controlling only one axis is designed, in order to solve the problem in a simpler architecture. Thus, modifications and improvements could be made at the next version of head stabilization platform. In order to implement an effective head stabilization platform both PID and LQR controllers are tested and compared in terms of their performances.

Three experiments are done by the SensoRHex robot at different speeds, angular velocity and acceleration changes of the robots body is measured by using an IMU. Performance of controllers with those signals are observed by giving the angular velocity as a reference to the platform and tracking ability is observed since if a system is able to track the state changes, it can cancel out those signals when they act as disturbance to the system.

Moreover, simulations of head stabilization platform with PID and LQR controllers are conducted in order to obtain responses at different conditions. Finally real experimental signals obtained from IMU at different experiments, are given to the head stabilization model as a reference and tracking ability of those controllers are observed. Although the main purpose of the study is to cancel the oscillations happens

on the angular velocity of the robot body, angle of the stabilization platform will be controlled with a less weight in the future.

Also effect of motor selection to the performance of the disturbance cancellation algorithm is purposed. And results with different motors during different robot speed are discussed. Moreover effects of different parameters like, sampling time, shuttle speed, illumination density and mounting angle of the actuator is observed in terms of controlling performance and motion blur in the received image data is discussed.

Results clearly shows that both controllers are successfully able to track the experimental data obtained during SensoRHex tests. Although their performances show great similarities an engineer must take more different parameters into consideration. LQR control requires the knowledge of the linearized state space model of the system in order to create the control parameters, on the other hand PID control does not require such things. So implementing a robust PID control is much simpler and requires less computational need than LQR controller, which could be considered as one of the reasons PID control still dominates the industry in spite of the fact that much more complex control algorithms are available. On the other hand one has the control over weight of the controller parameters as well as the control effort separately in the LQR controller.

Simulations with data measured on the robot during locomotion with different speed show that at the highest robot speed disturbance cancellation algorithms can not work as successful as the other speeds. So during image retrieving lowering the locomotion speed of the robot is recommended as a result of this study. Also by measuring the residual angular velocity at the top of the head platform in other words at the camera, one can simply reject the image data taken when there exists a disturbance which is higher than a certain value. By following those results a significant improvement in the image processing algorithms is suggested.

Since the manufacturing process of the planar head stabilization platform is still in progress, only simulation tests could be conducted at this study. But at the end of 2011 the hardware platform is planned to be completed. Then hardware test of this platform will be conducted initially. Also the design of a three axis head stabilization platform is almost complete and ready for manufacturing. While testing the

planar head stabilization model, tests will also be conducted on a three axis platform simultaneously.

In addition at this study only traditional control methods are studied as a start in controlling the disturbances occurred during legged locomotion. However as a future work, adaptive and predictive algorithms will be implemented and their performances will be compared with our robot SensoRHex.

REFERENCES

[1] Camera stabilization, 'http://www.redferret.net/?p=7468'.

[2] Head movements, 'http://www.conceptart.org/forums/showthread.php?p=1522574'.

[3] Isolation table, 2010, ' http://www.autom8.com'.

[4] Landseer enterprises, 'http://www.landseerllc.com/landseerpage9'.

[5] Minus k designs, 'http://www.minusk.com/'.

[6] A. A. A.-L. Abdullah I. Al-Odienat. The advantages of pid fuzzy controllers over the conventional types. *American Journal of Applied Sciences*, 5:653–658, 2008.

[7] R. Altendorfer, U. Saranli, H. Komsuoglu, D. E. Koditschek, J. H. B. Brown, M. Buehler, N. Moore, D. McMordie, and R. Full. Evidence for spring loaded inverted pendulum running in a hexapod robot. In D. Rus and S. Singh, editors, *Experimental Robotics VII*, Lecture Notes in Control and Information Sciences, chapter 5, pages 291–302. Springer, December 2000.

[8] K. Autumn, M. Buehler, M. Cutkosky, R. Fearing, R. J. Full, D. Goldman, R. Groff, W. Provancher, A. A. Rizzi, U. Saranli, A. Saunders, and D. E. Koditschek. Robotics in scansorial environments. *Proceedings of the SPIE,*, 5804:291–302, May 2005.

[9] K. Barya, S. Tiwari, and R. Jha. Comparison of lqr and robust controllers for stabilizing inverted pendulum system. In *Communication Control and Computing Technologies (ICCCCT), 2010 IEEE International Conference on*, pages 300 – 304, oct. 2010.

[10] G. A. Beals, R. C. Crum, H. J. Dougherty, D. K. Hegel, and J. L. Kelley. Hubble space telescope precision pointing control system. *Guidance, Navigation and Control Conference, Williamsburg, VA*, pages 50–56, Aug 18-20 . 1986.

[11] G. A. Beals, R. C. Crum, H. J. Dougherty, and J. L. Hegel, D. K.and Kelley. Hubble space telescope precision pointing control system. *Journal of Guidance, Control, and Dynamics*, 11:119–123, 1988.

[12] Beard, A. M., D. W. Schubert, von Flotow, and A. H. Practical product implementation of an active/passive vibration isolation system. *Vibration Monitoring and Control, Colin G. Gordon; Ed.*, 2264:38–49, 1994.

[13] G. Buckner, K. Schuetze, and J. Beno. Active vehicle suspension control using intelligent feedback linearization. In *American Control Conference, 2000. Proceedings of the 2000*, volume 6, pages 4014 –4018 vol.6, 2000.

[14] J. Debruin. Control systems for mobile satcom antennas. *Control Systems, IEEE*, 28(1):86 –101, feb. 2008.

[15] H. L. X. N. Dejun Sheng, Dapeng Fan. Bond graph approach to the modeling and simulation of a two-axis pointing and tracking system. *Mechatronics and Automation*, ICMA 2007:2337–2341, 2007.

[16] J. Diamond. Why animals run on legs, not on wheels. *Discover*, 4(9):64–67, September 1983.

[17] G. Gerson and A. Rue. Tracking systems. Eds. Dept. Navy: Washington, 1989.

[18] D. Goldman, H. Komsuoglu, and D. E. Koditschek. March of the sandbots. *Spectrum, IEEE*, 46(4):30–35, April 2009.

[19] D. A. Hilkert, James M.; Hullender. Adaptive control system techniques applied to inertial stabilization systems. *Proc. SPIE*, 1304:190–206, 1990.

[20] C.-I. Huang and L.-C. Fu. Smooth sliding mode tracking control of the stewart platform. In *Control Applications, 2005. CCA 2005. Proceedings of 2005 IEEE Conference on*, pages 43 –48, aug. 2005.

[21] N.-I. Kim and C.-W. Lee. High speed tracking control of stewart platform manipulator via enhanced sliding mode control. In *Robotics and Automation, 1998. Proceedings. 1998 IEEE International Conference on*, volume 3, pages 2716 –2721 vol.3, may 1998.

[22] S.-H. Lee, J.-B. Song, W.-C. Choi, and D. Hong. Position control of a stewart platform using inverse dynamics control with approximate dynamics. *Mechatronics*, 13(6):605 – 619, 2003.

[23] T. Lee, E. Koh, and M. Loh. Stable adaptive control of multivariable servomechanisms, with application to a passive line-of-sight stabilization system. *Industrial Electronics, IEEE Transactions on*, 43(1):98 –105, feb 1996.

[24] B. Li and D. Hullender. Self-tuning controller for nonlinear inertial stabilization systems. *Control Systems Technology, IEEE Transactions on*, 6(3):428 –434, may 1998.

[25] B. Li, D. Hullender, and M. DiRenzo. Nonlinear induced disturbance rejection in inertial stabilization systems. *Control Systems Technology, IEEE Transactions on*, 6(3):421 –427, may 1998.

[26] Y. Li, F. Marcassa, R. Horowitz, R. Oboe, and R. Evans. Track-following control with active vibration damping of a pzt-actuated suspension dual-stage servo system. In *American Control Conference, 2003. Proceedings of the 2003*, volume 3, pages 2553 – 2559, june 2003.

[27] H. Lin and J. McInroy. Adaptive sinusoidal disturbance cancellation for precise pointing of stewart platforms. *Control Systems Technology, IEEE Transactions on*, 11(2):267 – 272, mar 2003.

[28] G. N. R. P. Marc Raibert, Kevin Blankespoor and the BigDog Team. Bigdog, the rough-terrain quadruped robot. *Proceedings of the 17th World Congress The International Federation of Automatic Control*, 2008 July 6-11.

[29] M. Masten. Inertially stabilized platforms for optical imaging systems. *Control Systems, IEEE*, 28(1):47 –64, feb. 2008.

[30] A. N. K. Nasir, M. A. Ahmad, and M. F. Rahmat. Performance comparison between lqr and pid controllers for an inverted pendulum system. *INTERNATIONAL CONFERENCE ON POWER CONTROL AND OPTIMIZATION: Innovation in Power Control for Optimal Industry. AIP Conference Proceedings*, Volume 1052:124–128, 2008.

[31] J. J. Ortega. Gunfire performance of stabilized electro-optical sights. *Proc. SPIE 3692*, page 74, 1999.

[32] G. Ozdemir. Intelligent stabilization control of turret subsystems under disturbances from unstructured terrain. Master's thesis, METU, 2006.

[33] A. Preumont, M. Horodinca, I. Romanescu, B. de Marneffe, M. Avraam, A. Deraemaeker, F. Bossens, and A. A. Hanieh. A six-axis single-stage active vibration isolator based on stewart platform. *Journal of Sound and Vibration*, 300(3-5):644 – 661, 2007.

[34] M. Raibert. *Legged robots that balance*. MIT Press series in artificial intelligence. MIT Press, Boston, 1986.

[35] U. Saranli, A. A. Rizzi, and D. E. Koditschek. Model-based dynamic self-righting maneuvers for a hexapedal robot. *International Journal of Robotics Research*, 23(9):903–918, September 2004.

[36] A. Saunders, D. I. Goldman, R. J. Full, and M. Buehler. The rise climbing robot: body and leg design. In G. R. Gerhart, C. M. Shoemaker, and D. W. Gage, editors, *SPIE Unmanned Systems Technology VIII*, volume 6230, page 623017. SPIE, 2006.

[37] E. Sayginer, T. Akbey, Y. Yazicioglu, and A. Saranli. Task oriented kinematic analysis for a legged robot with half-circular leg morphology. In *Robotics and Automation, 2009. ICRA '09. IEEE International Conference on*, pages 4088 –4093, May 2009.

[38] B. Smith, W. Schrenk, W. Gass, and Y. Shtessel. Sliding mode control in a two-axis gimbal system. In *Aerospace Conference, 1999. Proceedings. 1999 IEEE*, volume 5, pages 457 –470 vol.5, 1999.

[39] M. J. Spenko, G. C. Haynes, J. A. Saunders, M. R. Cutkosky, A. A. Rizzi, R. J. Full, and D. E. Koditschek. Biologically inspired climbing with a hexapedal robot. *J. Field Robot.*, 25(4-5):223–242, 2008.

[40] Y. Su, B. Duan, C. Zheng, Y. Zhang, G. Chen, and J. Mi. Disturbance-rejection high-precision motion control of a stewart platform. *Control Systems Technology, IEEE Transactions on*, 12(3):364 – 374, May 2004.

[41] J. Tucker and A. de Sam Lazaro. Image stabilization for a camera on a moving platform. In *Communications, Computers and Signal Processing, 1993., IEEE Pacific Rim Conference on*, volume 2, pages 734 –737 vol.2, may 1993.

[42] C. Yang, Q. Huang, H. Jiang, O. O. Peter, and J. Han. Pd control with gravity compensation for hydraulic 6-dof parallel manipulator. *Mechanism and Machine Theory*, 45(4):666 – 677, 2010.

[43] F. Üzer. Camera motion blur and its effect on feature detectors. Master's thesis, METU, 2010.

[44] Özgür Hastürk. The stabilization of a two axes gimbal of a roll stabilized missile. Master's thesis, METU, 2011.